Title
Crossed Molecular Beams Study of O({sup 1}D) Reactions with H{sub 2} Molecules

Author
Miau, T.-T.

Publication Date
1995-05-01

LBL-37272
UC-401

Lawrence Berkeley Laboratory
UNIVERSITY OF CALIFORNIA

CHEMICAL SCIENCES DIVISION

Crossed Molecular Beams Study of $O(^1D)$ Reactions with H_2 Molecules

T.-T. Miau
(Ph.D. Thesis)

May 1995

Prepared for the U.S. Department of Energy under Contract Number DE-AC03-76SF00098

DISCLAIMER

LBL-37272

CROSSED MOLECULAR BEAMS STUDY OF $O(^1D)$ REACTIONS WITH H_2 MOLECULES

TZONG-TSONG MIAU
Ph.D. Thesis

DEPARTMENT OF CHEMISTRY
University of California, Berkeley

and

CHEMICAL SCIENCES DIVISION
Lawrence Berkeley Laboratory
University of California
Berkeley, CA 94720

MAY 1995

This work was supported by the Director, Office of Energy Research, Office of Basic Energy Sciences, Materials Sciences Division, of the U.S. Department of Energy under Contract No. DE-AC03-76F000981

Table of Contents

ACKNOWLEDGMENTS

It is only appropriate to start this acknowledgment with thanks to my adviser, Prof. Yuan. T. Lee. Only his kindness made everything possible for me. I am greatly indebted to Yuan for his generosity in accepting me as his student seven years ago and for his tolerance about my slow-moving behavior from then on. It was too late for me to realize how much I could have learned from him and the people surrounding him. His knowledge and enthusiasm about science is truly unmatchable. Now he is taking over the most difficult job in Taiwan, trying to elevate the scientific research in our country to a new dimension. I wish him the best.

This work could not be completed without the guidance of Dr. A. Suits, who, along with K. T. Lu, helped me set up the experiment and obtain the preliminary results. Equally helpful was XueMing Yang, who pushed me at the last stage of the experiment. I would also like to thank Prof. Piergiorgio Casavecchia from University of Perugia, Italy. He kindly provided me with his results on the same experiment prior to publication and commented on my work. Only with his data could I feel more confident with my own results.

During the eight years of stay at Berkeley, I came to know a lot of good friends, both inside and outside the Chemistry department. I am very grateful for their help and all the valuable things I learned from them. R. H. Tsaih in the IEOR department, Jason Wang, Weie Wang in the Nuclear Engineering department, and

Fred Chen in the Material Science department helped me settle down when I first arrived at Berkeley. They also taught me how to survive the first year as a foreign student and provided me with much advice about changing my major. Also to all my Chinese softball friends, it was truly fun to be able to enjoy a carefree Sunday afternoon playing games with them. In the chemistry department, in addition to all the supporting staff, many of the Lee group members also deserve special thanks. Bob Continetti, besides showing me how true scientific research was conducted, was the first one to point out that I should 'ask' him a question instead of 'axing' him. Pam Chu taught me how to operate the instruments in our group and many machining skills. James Chesko spent countless hours keeping our aging computers running, and he really helped me out when I was sick. Of course, he is also the (one and only) person who has shown me the wonder of 'Quantum Mechanics'. Laura Smoliar taught me how to deal with stress and 'trouble', and showed me what a wild American girl (oops, it should be woman) is like, and I am such a dinosaur in the space age. She also generously shared the cookies her mom made for her, which made me really miss home cooked meals (Thank you so much, Mrs. Smoliar). Of course, the cookies given to me by Cheryl Longfellow and Cindy Berrie are equally delicious. In addition, Laura, Cheryl and Jinchun Xie proofread my thesis and helped me with my poor command of the English language. Cheryl is also the main debugger of my computer programs and she had so many wonderful suggestions. I also enjoyed the time we had together, gobbling down all the jelly bellies. Domenico (Mimmo) Stranges is the other debugger of my program and he still owes me a meal of Chinese spaghetti. By the way,

Mimmo, one day I will prove to you that Italian pizza is also from China. There are many other people in this group, such as Su-Yu Chiang, Jingsong Zhang, Jim Myers, Hongtao Hou, Zhifeng Liu, Kun Liu, Floyd Davis, etc.; they all taught me something valuable. I will remember all of them for the years to come.

Of course, I will never be able to thank the staff here in the chemistry department enough. Without their expertise, graduate school would become a living hell for me. Yuan's three assistants, Ann Lawhead, Daina Tekorius, and Marian Grebanier, were most valuable when I had to deal with the bureaucracies. Since there are so many wonderful people in different parts of the department, I can only extend my gratitude to all of them and wish them the best. But one person I have to mention is Harry Chiladakis. Not only does he provide me (and the whole group) with valuable advice, but also he was the one who frequently visited me in the hospital when I was sick, and taught me many lessons about life. He even invited me to his family reunion parties, which allowed me to experience a different culture. Thanks, Harry (or Dad)!

It was totally unexpected to become a patient and have surgery here during my study. The surgery ordeal was adventurous, especially when I woke up finding that I had a big hole on my belly (or a hole on my big belly?). The visits from Harry and all the other people really boosted my morale. I'd also like to thank the people at the University Health Service, especially Andriana Schroenberg and Dr. S. Swanson. They provided me with the excellent health care when I was sick and continue to do so after that.

This acknowledgment won't be complete without mentioning two of my college professors, Prof. M. H. Young and Prof. C. T. Chang. Prof. Yang was the person who brought me into chemistry and paved the way for my change of major. His brother, Prof. Chang, kindly let me sit in his inorganic chemistry class and later introduced me to Yuan. The untimely death of Prof. Chang really saddened me. Even though I was never able to enjoy the richness and excitement in chemistry, I am grateful forever for their efforts in teaching and helping me.

Support from my parents and the rest of the family members is the only thing that has kept me going for the last several years. I will never be able to repay them for all the sacrifices they made for me. I will also forever remember three of my family members who passed away during the last eight years. I wish they rest in peace.

This work was supported by the Director, Office of Energy Research, Office of Basic Energy Sciences, Chemical Sciences Division, U.S. Department of Energy under Contract No. DE-AC03-76SF00098.

Abstract

Crossed Molecular Beams Study of $O(^1D)$ Reactions with H_2 Molecules

by

Tzong-Tsong Miau

Doctor of Philosophy in Chemistry

University of California at Berkeley

Professor Yuan T. Lee, Chair

The reaction dynamics of $O(^1D)$ atoms with H_2 molecules was reinvestigated using the crossed molecular beams technique with pulsed beams. The $O(^1D)$ beam was generated by photodissociating O_3 molecules at 248 nm. Time-of-flight spectra and the laboratory angular distribution of the OH products were measured. The derived OH product center-of-mass flux-velocity contour diagram shows more backward scattered intensity with respect to the $O(^1D)$ beam. In contrast to previous studies which show that the insertion mechanism is the dominant process, our results indicate that the contribution from the collinear approach of the $O(^1D)$ atom to the H_2 molecule on the first excited state potential energy surface is significant and the energy barrier for the collinear approach is therefore minimal. Despite the increased time resolution in this experiment, no vibrational structure in the OH product time-of-flight spectra was resolved. This is in agreement with LIF studies, which have shown that the rotational distributions of the OH products in all vibrational states are broad and highly inverted.

INTRODUCTION

Reactions involving electronically excited oxygen atoms, $O(^1D)$, play an important role in atmospheric chemistry[1] as well as in combustion processes. Among those reactions, the reaction

$$O(^1D) + H_2(^1\Sigma_g^+) \longrightarrow OH(^2\Pi) + H(^2S_g) \qquad \Delta H = -43.5 \text{ kcal/mole}$$

has received a great deal of attention for various reasons. The OH product from this reaction can further react with ozone, which contributes in part to the depletion of stratospheric ozone. In addition, this reaction is closely connected to the decomposition of water during high temperature combustion. For those who study chemical dynamics, this reaction is a prototype for reactions in which the reactants can form a complex (in this case H_2O), in contrast to reactions such as $F + H_2 \longrightarrow HF + H$, where a direct reaction pathway without complex formation is believed to be dominant.[2] Therefore by studying how this reaction proceeds, it should be possible to provide valuable information about the dynamics of these types of complex-forming reactions. Also, because of the excess energy ($\approx$ 7 eV) during the complex formation, this reaction can probe the upper part of the ground state potential energy surface of water, which in recent years has become the subject of spectroscopic studies because of its potentially simple spectroscopic features. Another reason for studying this reaction is its possible application to

chemical lasers,[3-5] because the internal energy distributions of the OH products are highly inverted, both vibrationally and rotationally. Extensive studies have been done on this reaction and related systems, both experimentally[3-19] and theoretically,[21-31] and a vast amount of information is available. Despite extensive research, not all aspects of the dynamics of the reaction are well known and sometimes contradictions arise, leading to confusion about the true nature of this system.

Kinetic studies on this system[6,7] show that the reaction rate constant of this reaction is in the range of 1.3 - 2.7 x 10^{-10} $cm^3molecule^{-1}s^{-1}$ at room temperature, which is nearly gas kinetic (i.e., almost all collisions are reactive) and very few collisions will lead to the quenching of the oxygen atoms from ^1D to ^3P states. DeMore[6] further showed that this reaction proceeded with essentially no activation energy, implying that the potential energy surface involved was entirely attractive. More recent studies on this system mainly involve the determination of the energy distribution of the products. For this reaction, because of the large exothermicity, up to $v' = 4$ in OH vibration is accessible at room temperature conditions. Using laser induced fluorescence (LIF),[8,10-13] the rotational distributions in the OH $v' = 0$ - 3 vibrational states were determined to be highly inverted, with little population at lower rotational levels. In addition, results[13,18] showed a pronounced preference for the lower OH Λ-doublet component (Π^+) at high rotational states. However, because of the existence of the upper Λ-doublet component (Π^-), the possibility of surface hopping has been suggested between $O(^1D) + H_2$ and $O(^3P) + H_2$ surfaces in the entrance channel, as observed in similar reactions between $O(^1D)$ and

hydrocarbons.[18] The full vibrational distribution of the OH product was first investigated by Butler *et al.*[14] using the low pressure infrared chemiluminescence technique and it was found to be inverted as (P(v'=0:1:2:3:4) = 0.22:0.20:0.23:0.22:0.13). Similar conclusions were reached by Aker *et al.*[15] using time-resolved Fourier transform spectroscopy. Huang *et al.*[4] and Shao *et al.*[5] applied the grating selection chemical laser technique to study the vibrational distribution; they obtained similar distributions from v' = 1 to 4, but the overall distribution was still peaked at v' = 0. Matsumi *et al.*[19] studied the translational energy release of this reaction by measuring the Doppler profile of the H atom product using the resonance enhanced multiphoton ionization (REMPI) method. They concluded that about 30% of the available energy (E_{avail} = 45.5 kcal/mole) went into translational motion. In order to determine the exact nature of this reaction, studies of $O(^1D) + HD \longrightarrow H(D) + OD(OH)$ reaction were carried out to determine the isotopic branching ratio of this reaction. By monitoring both the hydrogen and deuterium atom products by VUV laser induced fluorescence, Tsukiyama *et al.*[16] obtained a H/D ratio slightly greater than one (1.13 ± 0.08). While Butler *et al.*[12] claimed similar results after integrating the available OH rotational and vibrational state population from their LIF results, their data suggested otherwise.[20] So far, only one crossed molecular beam study of this reaction has been published,[17] and the result suggested an insertion mechanism with a forward-backward peaked center-of-mass angular distribution. The symmetric angular distribution was attributed to the homonuclear nature of the reactant H_2 instead of taking this as evidence that long lived complexes were

formed. The translational energy release found in that study is peaked around 10-12 kcal/mole (vs. E_{avail} = 46 kcal/mole), which is consistent with the LIF and Doppler profile studies that show most of the available energy is deposited in vibrational and rotational motion. By comparing the vibrational and rotational energy distributions of the OH products with statistical theories such as RRKM and phase space theory, it has been concluded that this reaction does not involve long-lived complexes, but rather proceeds on the time scale of a few vibrational periods and possibly less than one rotational period of the water complex. On the other hand, the slightly greater than one H/D ratio suggests the formation of long-lived complexes.

Theoretical treatment of this reaction generally involves classical[21-23] or quasi-classical[24-29] trajectory studies of this system, and only one quantum reactive scattering study with reduced dimensionality is available.[30] Even though this system only involves eight valence electrons, more accurate quantum treatment is still not available because of the large amount of excess energy and the possible involvement of several potential energy surfaces. So far, most studies have been concentrated on the ground state potential energy surface, with a few exceptions.[28,29] Several ground and excited state potential energy surfaces were built based upon available empirical data, *ab initio* calculations and the valence bond diatomics-in-molecule (DIM) method.[32] Two reaction pathways were proposed for this reaction: (1) insertion of the $O(^1D)$ atom into the hydrogen molecule to form a short-lived complex and (2) direct abstraction of one hydrogen atom from the hydrogen molecule by the oxygen atom via a near collinear

approach. The insertion mechanism is believed to be purely attractive in the entrance channel without any barrier, while the abstraction pathway possesses an entrance barrier; however, results from various studies cannot agree on the barrier height. For most theoretical calculations, regardless if there is a potential energy barrier for the collinear approach or not, they all indicate that the $O(^1D) + H_2$ reaction occurs predominantly by the insertion mechanism with the complex falling apart promptly. The shapes of the OH product rotational energy distributions obtained in all the calculations in general compare well with the experimental results, but agreements between the OH vibrational distributions are thus far less than satisfactory. In addition, the calculated center-of-mass angular distributions of the OH product vary from one study to another. To resolve the inconsistencies between the theoretical and experimental results on the OH vibrational distribution, Kuntz *et al.*[28,29] pointed out that if more than one potential energy surface was involved in this reaction and the collisional energy was enough to overcome the energy barrier on the first excited state surface, the contribution from the collinear geometry on the first excited state energy surface could become significant and have an effect on the final OH vibrational state distribution. It was also noted in their study that this reaction probably was more susceptible to the quantum effect since there were two hydrogen atoms in this system and the only quantum scattering study[30] showed more vibrational excitation than its classical counterpart[22] using the same potential energy surface. Therefore, they suggested that a detailed quantum scattering study of this system might be more appropriate. Early attempts to explain the highly inverted rotational distribution of the OH

products concentrated on the incomplete energy redistribution in the complex. However, Monte Carlo simulations done by Rynefors *et al.*[33,34] showed that this deviation could be attributed to the constraint of angular momentum conservation at the transition state instead of a specific dynamical effect, assuming this reaction indeed formed a long-lived complex. Once they included this constraint in the context of RRKM theory, they were able to reproduce the inverted rotational energy distribution results from LIF studies and the laboratory angular distribution obtained from the crossed molecular beams experiment. However, the vibrational energy distribution they reported was still peaked at $v' = 0$, as expected from a regular statistical theory. In addition, they failed to note that the lifetime of the water complex obtained from trajectory studies was too short to apply RRKM theory for the analysis.

In summary, the consensus so far is that this reaction proceeds mainly through an insertion process but without forming a long-lived complex. The direct abstraction pathway only contributes to a small extent in all the reactions. In addition, the inversion of the OH vibrational energy distribution is the result of dynamical effects and is most sensitive to changes in the potential energy surfaces.

The purpose of this study is to reinvestigate this reaction by the crossed molecular beams technique with improved oxygen beam conditions and better time resolution. A previous study of this reaction[17] used an rf discharge to generate the $O(^1D)$ atomic beam, which had comparable velocity to the H_2 beam but with a rather wide beam spread(~20%). The fast oxygen beam velocity had the undesirable effect of limiting the OH products to a narrow range of laboratory

angles. The poor $O(^1D)$ beam speed ratio also smeared out any possible features in the angular distribution and the time-of-flight (TOF) spectra. In addition, the flight length of the neutral molecules was only ~17 cm, and the multichannel scaler resolution used was limited to 12 μsec per channel because a cross-correlation chopper was used to sample the products. The poor time resolution and short flight length caused the spectra to be congested into only a few channels (typically less than 10 points per spectrum). The center-of-mass flux-velocity contour map of the OH product obtained from deconvolution of the raw data also suggested slightly more backward scattered intensity, which indicated that the insertion mechanism might not completely describe this reaction. Because of all the reasons mentioned above, the result obtained in that study cannot be taken as conclusive. Another reason to reinvestigate this reaction is that the OH molecules have a vibrational spacing of ~ 3500 cm^{-1} (10 kcal/mole). With better defined beam conditions (slower oxygen atom beam velocity and higher speed ratio) and a longer flight length, it might be possible to resolve vibrational structure, as in the case of the $F + H_2 \longrightarrow HF + H$ reaction.[2] Furthermore, it will be extremely useful if the same experiment can be carried out on the $O(^1D) + HD$ reaction. From the translational energy releases of the two product channels (OH+D/OD+H), it should be possible to obtain a crude estimate of the isotopic branching ratio using information theoretical treatment,[35,36] which can shed some light on the dynamics of this reaction.

Unlike most of the crossed molecular beams experiments in which two continuous beam sources are used, in this experiment both beams are formed using

pulsed nozzles to produce more intense beams. The $O(^1D)$ atomic beam is produced by photodissociating ozone molecules at 248 nm. With carefully chosen ozone beam condition, an intense $O(^1D)$ beam with a beam spread of ~ 8% or better can be achieved. The success of this source will be useful in future to studies of other important reactions such as $O(^1D)$ + HCl and hydrocarbons, and the same design can be applied to the production of other pulsed radical beams.

EXPERIMENTAL

The basic design of the universal crossed molecular beams apparatus used in this experiment and its working principles can be found in the literature[37], so it will only be briefly discussed here. Slight modifications were made in order to use two pulsed valves and the resulting configuration is shown in Fig. 1. It is similar to the setup used in the D + H_2 experiment[38] several years ago with some major differences in the oxygen atomic beam source geometry. First of all, since the $O(^1D)$ atoms have a wide range of velocities and are randomly scattered in space following the photodissociation of the ozone molecules, further expansion and collimation of the $O(^1D)$ atoms is needed. The precursor beam (ozone seeded in helium) was directed towards the collision chamber in order to provide further expansion and to carry the $O(^1D)$ atoms into the interaction region. Secondly, there were no differential pumping regions installed in either source regions. The nozzle-to-skimmer distance was found to give an undisturbed beam profile and optimum intensity at 12-16 mm (For more details, see Appendix A) and 12 mm was used. The skimmer had a 50°/60° geometry with a 1 mm opening. Inside the collision chamber, a 0.13 mm thick stainless steel mechanical chopper (17.8 cm in diameter) with four 0.75 mm wide slots was placed in front of the skimmer and about 2 cm upstream from the interaction region to reduce the pulse width of this beam to about 7 μsec (@200 Hz chopper frequency). The photodiode signal

triggered by the chopper wheel served as the time reference throughout this experiment.

The $O(^1D)$ atomic beam was generated by photodissociating ozone molecules with a KrF excimer laser ($\lambda = 248$ nm). The photodissociation of ozone molecules by ultraviolet radiation around 250 nm has been studied extensively in the past and it will not be discussed here. One is referred to Ref. 39 and 40 for details. In short, the absorption of a photon at 248 nm by an ozone molecule is very efficient ($\sigma \approx 1.07 \times 10^{-17}$ $cm^2 molecule^{-1}$), and most of the absorption leads to the dissociation products $O(^1D)$ and $O_2(^1\Delta)$. Since the absorption is easily saturated, the laser power is not a crucial issue in this experiment. Typical laser powers used were in the range of 150 - 200 mJ/pulse before entering the chamber, but a significant portion was lost before it reached the pulsed valve because of the laser beam divergence. The typical amount of ozone depletion obtained in the chopped pulse was around 25 - 30%.

Two cylindrical quartz lenses with 19 cm focal length were used to focus the light to a ~ 1 mm x 1 mm spot about 0.5 mm downstream from the pulsed valve nozzle. The dissociation of the ozone molecules occurred during the expansion process and a portion of the $O(^1D)$ atoms produced from dissociation remained in the same gas pulse and went through further expansion. Helium gas was used as the carrier gas throughout this experiment so that the quenching of $O(^1D)$ atoms was minimized.

The piezoelectric pulsed valves used for both sources were based upon Proch and Trickl's design.[41] For the $O(^1D)$ beam, a short plunger made of

aluminum was used so that the opening and closing time of the pulsed valve could be shortened, which in turn resulted in a shorter gas pulse. The opening of the nozzle was 0.5 mm in diameter. During initial experiments, a Viton O-ring coated with Teflon was used as the plunger seal, but it was soon discovered that the O-ring became swollen shortly after coming in contact with ozone, making the valve inoperable. A switch was made to a Teflon O-ring, but the result was unsatisfactory due to the lack of elasticity in the Teflon material. Finally, a Kalrez O-ring was chosen, and it proved to be ozone resistant and a reasonably good elastomer. For most of the experiments described below this pulsed valve was activated by an 80 μsec, -320 V (peak voltage) pulse with 3.5 μsec rising and falling time constants.

The ozone used in this experiment was generated by a commercially available ozonator. The output of the ozonator, containing about 10% ozone, was passed through a nickel coated stainless steel trap filled with coarse silica gel. This trap was placed in dry ice/acetone slush (temperature = -78°C) during the ozone making process to help the adsorption and also for safe storage whenever it was not in use. Before running the beam, the trap was filled with helium and pumped out. This was repeated several times to remove residual O_2 gas in the trap and it was carried out while the trap was still in the slush so the ozone would remain adsorbed to the silica gel. When running the beam, the trap was transferred to a thermostatically controlled variable low-temperature bath, and helium gas was used to carry the desorbing ozone out of the trap. The total stagnation pressure of the O_3/He mixture was kept at 30 psig. The temperature of

the cooling bath was carefully controlled such that the concentration of the ozone molecules in the gas mixture was around 1% (equivalent to ~23 torr of O_3 in the gas mixture). To monitor the ozone concentration, 500 torr of the gas mixture was leaked into a 1 cm x 1 cm quartz flow cell from time to time, and the ultraviolet absorption of the gas mixture at 280 nm was measured. Typically, it took about one to two hours before the ozone beam became steady. Some O_2 molecules remained in the beam in spite of the purging and flashing of the trap at the beginning. This mainly resulted from the residual O_2 in the trap and thermal decomposition of the O_3 molecules in the gas line before entering the source chamber. This posed no serious problem for the experiment under study. Very minute amounts of ozone dimers were also observed in the mass spectra. Since they would be easily broken into smaller species when the laser interacted with the beam, the pulsed valve nozzle was not heated throughout the experiment.

For the H_2 beam, a pulsed valve with a 7 cm long plunger was used. The nozzle diameter was 0.75 mm and the skimmer to nozzle distance was set around 15 mm. The valve was driven by an 80 μsec, -320 ~ -360 V(peak voltage) pulse with 3.5 μsec rising and falling time constants. High purity normal H_2 gas (99.995%) was used without further purification. Because the valve body was in contact with the differential wall, this pulsed valve became colder and easier to open (i.e. requiring lower driving voltage) when the main chamber cold shield was cooled down to liquid nitrogen temperature. As a result, slight heating was applied on the valve body to keep it at 300K. After the gas had been running through the valve for a period of time, the temperature of the valve became higher

and the valve started to close. The driving voltage was then adjusted to keep the source chamber at a constant background pressure (~ $4x10^{-5}$ torr). The temperature change during the course of the experiment was found to be around 7K, which in turn translated into a 1.5% change in the beam velocity. The H_2 beam velocity used in this study was 2700 m/s, with a speed ratio of 12.1.

Due to the fact that oxygen has stable isotopes at masses 17 and 18, time dependent backgrounds at m/e = 17 and 18 were inevitable. It was also noted that there were trace amounts of water in the ozone beam, although its origin was not clear. To cut down the time dependent background, a collimation slit (2 mm x 2 mm) was installed ~ 0.5 cm in front of the chopper wheel. In addition, a cryogenic copper cold panel at liquid nitrogen temperature was placed around the collision zone facing the detector to further reduce the unwanted background.

The experiment was carried out by spinning the chopper wheel at 200 Hz, and the photodiode signal coming from the chopper wheel (4 x 200 Hz = 800 Hz) was divided by 8 and split into three secondary triggers. Two out of those three triggers were then separately delayed, and sent to the pulsed valves which were operated at 100 Hz. The third trigger was further divided by 2, delayed, and sent to the photolyzing laser. The various delays could be changed independently of each other with respect to the photodiode signal. Fig. 2 shows the timing relationships between all the triggers and their typical values. The delay of the ozone beam with respect to the chopper wheel was determined by finding the peak of the ozone pulse. The intensity of the peak stayed roughly the same within about 30 μsec, and the center was then chosen. The laser trigger was adjusted so that a

maximum increase of signal was obtained at m/e = 8 (O^{2+}). The increase of O^{2+} signal was taken as an indication that O(^{1}D or ^{3}P) atoms were produced. The O(^{1}D) beam velocity and its speed ratio were determined based on the O^{2+} time-of-flight spectra. The delay between the two pulsed beams was found to be critical and had to be carefully chosen. For details on how this delay can distort the experimental results, one is referred to Appendix B. As a result, the delay of the H_2 beam was chosen so that the O(^{1}D) beam intersected the H_2 beam at the front part of the pulse, close to its peak.

Out of the two products (H and OH), the hydrogen product was very hard to detect because of the high m/e = 1 background in the detector and its extremely fast velocity. Therefore, the scattered OH products were detected by using a quadrupole mass spectrometer rotating around the center of the interaction region. The detector was triply differentially pumped by ion pumps and turbomolecular pumps and maintained under ultrahigh vacuum conditions. The ionizer region was further cooled to liquid nitrogen temperature to remove any condensable gases. Once the molecules entered the detector, they were first ionized and then mass selected. These mass selected ions were then detected by a Daly type ion counter.[42] The signals, after being amplified and discriminated, were sent to a custom made 4096-channel multichannel scaler (dwell time set at 4 μsec per channel), triggered by the same pulse used to trigger the laser. The resulting time-of-flight spectra contained both the laser on and laser off signals, separated by 10 milliseconds (2500 channels). Spectra were taken at as many as 19 different laboratory angles. The laser correlated spectra were obtained by subtracting the

laser off signals from the laser on signals. The laboratory angular distribution of the OH product was obtained by repeatedly taking TOFs at three or four different angles at a time with a fixed laboratory angle as the reference, usually 15 degrees from the oxygen atomic beam. The laser correlated signals were then integrated and normalized with respect to the reference angle intensity. All the data collection process was controlled by an LSI 11/73 microcomputer and then transferred to PCs for further analysis.

RESULTS AND ANALYSIS

Production of the $O(^1D)$ atomic beam

A major consideration in this experiment is to produce and monitor the $O(^1D)$ atomic beam. Since it was not possible to measure the $O(^1D)$ beam at m/e = 16 directly because of the existence of the ozone and oxygen molecules, in order to obtain the $O(^1D)$ beam velocity, the signal at m/e = 8 (O^{2+}) was monitored in the experiment. This is based on the assumption that the $O(^1D)$ atoms should produce more doubly charged oxygen ions than the undissociated ozone molecules. Fig. 3a shows the O^{2+} signal with and without the photolyzing laser. The increase in the O^{2+} signal was significant and as much as a 400% increase in the O^{2+} could be observed under optimum conditions. To obtain the $O(^1D)$ beam velocity, the laser off signal was first scaled according to the amount of depletion observed in the ozone (m/e = 48) signal, then subtracted from the laser on signal. Fig. 3b shows the subtracted O^{2+} spectrum and its corresponding fit, assuming a supersonic beam velocity distribution.[43,44] As shown in this figure, the fit somewhat underestimated the fast edge. The appearance of this fast leading edge can be attributed to two possible reasons: (1) local heating of the beam pulse by the photolyzing laser and (2) incomplete supersonic expansion of the $O(^1D)$ atoms. A fast edge caused by the first process was also observed in the time-of-flight spectrum of the remaining ozone beam. Therefore the fast edge in the O^{2+} TOF spectrum also contained contributions from the fragmentation of the ozone molecules in the ionizer.

Although the second cause cannot be ruled out completely, it is highly unlikely since if the expansion is not complete, the $O(^1D)$ atoms will scatter in all directions and the possibility of staying in the pulse is therefore minimal.

If the fast edge was neglected in the beam velocity calculation, an $O(^1D)$ beam velocity of ~ 1790 m/s with a speed ratio of ~ 11.9 was obtained. This beam velocity, when used in the data analysis of the $O(^1D) + H_2$ experiment, was found to be slower than it should be. A more adequate beam velocity was determined to be around 1900 m/s. Besides the fact that this discrepancy can be attributed to the negligence of the fast edge as mentioned above, it can also be caused by the inappropriate use of the O^{2+} signal to calculate the $O(^1D)$ beam velocity. Since the O_2 products coming from the dissociation usually contain a significant amount of internal energy (including electronically excited oxygen molecules), it is possible that the slow part of the O^{2+} signal comes from the fragmentation of those oxygen molecules in the ionizer. However, due to lack of information on the cracking patterns of the highly excited oxygen molecules and their exact composition in the beam, this correction could not be made. Therefore, the estimated value of 1900 m/s for the $O(^1D)$ beam velocity was used in the analysis of the $O(^1D) + H_2$ reaction.

$O(^1D) + H_2 \longrightarrow OH + H$ Reaction

Fig. 4 shows the Newton diagram for this reaction. The solid circle represents the absolute maximum center-of-mass velocity the OH products can acquire from this reaction, and the dashed circles represent the maximum center-

of-mass velocities the OH products can have when produced in different vibrational states other than $v' = 0$. The center-of-mass angle of this system is at 10 degrees. Although the absolute maximum Newton circle spans from -33 degrees to 54 degrees in the laboratory frame, signal was only observed between -15 and 40 degrees. Beyond this range, the signal was either too weak to be observed or beyond the detector's reach (the detector can swing between -17.5 and 60 degrees).

To analyze the data, a forward convolution algorithm was used to obtain the unscaled total reaction cross section $I_T(\Theta,E_t)$ in the center-of-mass frame, where Θ is the center-of-mass scattering angle and E_t is the products' translational energy release. For reactions with only one product channel, if there is more than one reaction mechanism involved, or the product(s) can populate a number of vibrational states, the $I_T(\Theta,E_t)$ can be written as a weighted sum of several independent components, $I_i(\Theta,E_t)$. Here *i* can represent contributions from different reaction mechanisms or vibrational states. In general, however, this separation is arbitrary. It is then assumed that each of those components has an energy-angle separable form and can be written as the product of a translational energy release distribution function $P_i(E_t)$ and center-of-mass angular distribution function $T_i(\Theta)$, namely, $I_i(\Theta,E_t) = P_i(E_t)\cdot T_i(\Theta)$. Therefore, the total reaction cross section $I_T(\Theta,E_t)$ can be expressed as $\sum_i w_i \cdot P_i(E_t)\cdot T_i(\Theta)$, where w_i is the contribution (or the weighting factor) from the *i*th component. If there is only one component, the $I_T(\Theta,E_t)$ is reduced to the usual uncoupled form $P(E_t)\cdot T(\Theta)$. Presumed point form $P_i(E_t)$s and $T_i(\Theta)$s were used to simulate the OH product

time-of-flight spectra and its laboratory angular distribution, taking into account both beams' angular and velocity spread, the finite ionizer length and the necessary coordinate transformation. The effect of the finite detector aperture was not considered in the analysis. In addition, since this reaction is exothermic and believed to proceed without any energy barrier, an $E^{-1/3}$ collisional energy dependence of the reaction cross section was used to provide an additional weighting for the collisional energy spread. Comparisons were then made between the simulated results and the experimental data and the w_is, $P_i(E_t)$s and $T_i(\Theta)$s were adjusted accordingly until a satisfactory fit was obtained. The FORTRAN program used in the analysis originated from R. Buss[45] and was modified and ported to PCs. All data manipulation and analysis were carried out on an Intel 486DX based personal computer.

Fig. 5 shows time-of-flight spectra taken at m/e = 17 with and without the photolyzing laser at several laboratory angles. When the detector is within 20 degrees of the oxygen atomic beam, there are peaks uncorrelated with the laser, so subtraction is required in order to obtain the laser correlated signal. From the shapes of the laser off spectra at different angles and the fact that the background does not go away before 20 degrees, it is speculated that there are two origins of the background signal. One is probably due to scattering of the water molecule impurity in the oxygen beam off the hydrogen molecule, which then fragments to m/e = 17 in the ionizer (e.g. 15 degrees). It is also possible that the $O(^3P)$ atoms scatter off the hydrogen molecules unreacted and then are detected at m/e = 17 due to mass leak. (Oxygen also has stable isotope at mass 17). The second process, if

it exists, will pose a serious problem for the background subtraction since the photolyzing laser will also produce oxygen atoms in the ^3P state at the same time the $O(^1D)$ atoms are produced, in addition to the original minor amount of $O(^3P)$ atoms in the ozone beam. The background from those two processes is mainly limited to between 0 and 20 degrees due to their kinematics. Another origin of the background is from the beam itself and its effusive background (e.g. -5 degrees). It is the major contribution to the background when the detector is placed very close to the oxygen atom beam (≤10 degrees). The peak directly from the beam is slower than the forward scattered peak from the water scattering process and when superimposed on the scattered water peaks, it causes broadening of the fast peak (e.g. 10 degrees). The effusive background is usually very slow and does not contribute very much to the background. Bear all those possible causes in mind, the major problem that arises from this time dependent background is the large uncertainty in the OH product laboratory angular distribution near the oxygen beam and the associated TOF spectra. This problem is further complicated by the use of a photolyzing laser. When the laser is on, the gas pulse will be slightly faster due to the heating. Therefore, the background peak position and even the profile will be slightly different in the laser on and laser off spectra. Hence the subtraction is by no means a trivial task. Since the background signal mainly comes after the major part of the true signal, the influence of the subtraction will only affect the determination of the slow component of the OH product, which in this reaction should only account for a small percentage of the total reaction. The subtraction to obtain the laser correlated signal is therefore carried out directly

without further scaling. The resulting time-of-flight spectra, as shown in Fig. 7, do not show any obvious structure, as opposed to the results obtained in the F + H_2 experiment.[2]

The OH product laboratory angular distribution, obtained by integrating the laser correlated signals and then scaled to a common angle (15 degrees), is shown in Fig. 6, and it also does not show any obvious structure. The intensities at 17.5 and 22.5 degrees, although consistently high throughout the experiment, are still within our experimental uncertainty. The typical uncertainty of the distribution is about $\pm$10%, which is larger than that of the previous study. This is in part due to the reduction of the sensitivity by using a longer flight length for the neutral molecules in this experiment, and partly due to the necessity of background subtraction near the oxygen beam as mentioned before. Another major factor that can affect the accuracy of this distribution (and the TOF spectra) comes from the background scattering events and is described in Appendix B. Because the collisional energy used in this study (2.3 kcal/mole) was similar to that used in the previous experiment (2.71 kcal/mole),[17] it was expected that the same $P(E_t)$ and $T(\Theta)$ should fit these results. However, it was soon found that the old $P(E_t)$ and $T(\Theta)$ fit poorly with the experimental laboratory angular distribution (the dotted line in Fig. 6) and when compared with the experimental time-of-flight spectra, the backward scattered intensity with respect to the $O(^1D)$ beam should have been more broadly distributed instead of being peaked narrowly along that direction. Being narrowly peaked at the exact backward scattered direction caused the simulated time-of-flight spectra to be doubly peaked at large laboratory angles

(around 20° - 35°), and the simulated peak was slower than the experimental data. The reason that this double peak feature did not show up in the previous study is because of their poor time resolution and the fast oxygen beam velocity, and therefore all the products were coalesced into a few channels. Unless there were systematic errors involved in our data collection process, it could only be explained by the inadequacy of the old $P(E_t)$ and $T(\Theta)$. Thus the form of $P(E_t)$ and $T(\Theta)$ had to be modified. Linear combination of two sets of $P(E_t)$s and $T(\Theta)$s were used to obtain a satisfactory fit to our experimental data. Fig. 6 shows the fit to the laboratory angular distribution (the solid line) and Fig. 7 shows the fit to several time-of-flight spectra. The translational energy distribution was separated into a fast (Fig. 8) and a slow (Fig. 9) component. This separation was done because the slow products might have larger uncertainties due to the background subtraction. The fast component has an angular distribution that is broadly backward peaked with respect to the $O(^1D)$ beam, with a possible dip in the exact backward direction. It also has some contributions in the forward scattered direction. This component accounts for ~90% of the total reaction.[46] Its $P(E_t)$ is broader compared to the previously used $P(E_t)$ but peaks around the same position. The slower component, on the other hand, has a nearly isotropic center-of-mass angular distribution, which slightly favors the forward direction.

As shown in Fig. 7, the fit to the time-of-flight spectra near the center-of-mass angle is less than perfect. As mentioned earlier, it all happens near where the background subtraction becomes necessary and corresponds to the low translational energy release component. In addition to attributing this mismatch to

the large uncertainty in the spectra, the effect of the finite detector aperture, which is neglected in the fitting process, should be considered. Taking this effect into account should be able to smooth the resulting fit and obtain better agreement with the experimental data. Another conceivable reason for this mismatch is the use of a smooth $P(E_t)$ for the slow component. The OH molecule has a rather large rotational constant (~ 18 cm^{-1}), and the low translational energy release means high rotational excitation for the OH product in low vibrational states ($v' = 0$, 1, or 2). Thus, the energy spacing between adjacent high rotational levels can be as large as 3 kcal/mole and exceed the collisional energy spread. Therefore it might not be appropriate to use a smooth $P(E_t)$ for the fitting process. However, attempts to use a smooth $P(E_t)$ with some discrete peaks to account for those rotational levels did not improve the fit.

Since in this experiment the OH products spread out more in space due to the use of a slower $O(^1D)$ beam, the sensitivity of this experiment is somewhat lower than that of the previous experiment. Therefore, the contribution from the products with the highest translational energy release cannot be accurately determined. The simulated laboratory angular distribution and TOFs are not very sensitive to the $P(E_t)$ contribution beyond ~ 35 kcal/mole, where only the OH products with $v' = 0$ and low j's can be populated, even though the total energy available is 46 kcal/mole. However, if the contribution in this energy region is not zero, it will give a faster rising edge for the spectra near the center-of-mass angle than the ones obtained in the experiment. Therefore, it is not expected that this energy range will contribute significantly to this reaction. This also agrees with

earlier results on the internal energy distribution of the OH product; there most of the OH molecules were rotationally highly excited, with very little population at low j' values.

Fig. 10 shows the OH product flux-velocity contour diagram constructed from the two sets of translational energy release distributions and center-of-mass angular distributions. As mentioned earlier, this study shows more backward scattered OH products than the forward scattered ones. Another major difference between our results and the results from the previous study is that in this work the peaking in both forward and backward directions is not as strong. The ratios of intensity at 90° to that on the relative velocity vector are T(90°)/T(0°) = 0.67 and T(90°)/T(180°) = 0.56, respectively. Previously both of those values were 0.33. However, in general, our contour map resembles in shape with the direct deconvolution result obtained in the previous study.

Before we go on to explore the possible implications of our experimental results on the dynamics of this reaction, it is important to ask the following question: Is it possible to fit our data in terms of two center-of-mass angular distributions with one having the forward and backward symmetry? The reason for doing so is that in most cases, this reaction occurs through the oxygen atom attacking the hydrogen molecule sideways to form a short-lived complex, and because of the homonuclear nature of the hydrogen molecule, the center-of-mass angular distribution should show a forward and backward symmetry. On the other hand, if the oxygen atom attacks the hydrogen molecule in a collinear fashion and the reaction happens through direct abstraction, the angular distribution usually

shows an asymmetric, or more precisely a backward peaked profile. Being able to separate the angular distribution into those two parts, it will be valuable for understanding the dynamics of this reaction. By examining the fit of the fast and slow component, it seems the only way to achieve that goal is to assume an isotropic (or even sideways peaked) center-of-mass angular distribution for the symmetric component. However, the results obtained so far have large deviations from the experimental data and again, unless we have more confidence in the data near the oxygen atomic beam, the separation of this reaction into a symmetric and an asymmetric component will be a difficult task.

DISCUSSION

In order to explain the dynamics of this simple reaction, it is essential to understand the possible potential energy surfaces involved. Fig. 11 shows the energy correlation diagram of the $O(^1D,^3P) + H_2$ system for the low lying states.[47] When the $O(^1D)$ atom approaches the hydrogen molecule, depending on the direction of the approach, initially the oxygen atom can interact with both hydrogen atoms at the same time or with only one of them. The first case is characterized as the lateral attacking or insertion process, and as the reactants approach each other the potential energy surface manifold splits into five surfaces. If the approach is in C_{2v} configuration, the reaction intermediate is directly correlated with the $^1A_1$ ground state of water molecule (or $^1A'$ in C_s symmetry). This part of the surface is purely attractive and has a very deep well, so a collision complex can exist. Unlike the ground state surface, all the excited states have barriers with respect to the reactants $O(^1D)$ and H_2 and are not energetically accessible for reactions under thermal conditions. Therefore, reactions involving the oxygen atom attacking the hydrogen molecule laterally occur entirely on the ground state surface of water. In the second case, where the oxygen interacts with only one H atom, if the approach is exactly collinear ($C_{\infty v}$), the degeneracies are lifted, resulting in three surfaces (Σ,Π,Δ). As predicted by theory[29,32d], the Σ surface is attractive, the Π rises up slightly exhibiting a small barrier, and the Δ state is totally repulsive and therefore irrelevant to this discussion. Because the

ground state of the OH product is a Π state, at some later point along the reaction path, the Σ surface must eventually rise up to cross the Π surface. The reason is that the Σ state correlates with the first excited state of the products, $OH(A^2\Sigma^+)$ + H, whereas the Π state correlates with the ground state, $OH(X^2\Pi)$ + H. When the approach is off the collinear geometry, those two surfaces form an avoided crossing, but they will remain energetically accessible as long as the O-H-H bond angle is larger than 150° (near collinear geometry). For a strictly collinear approach, the Σ state will prevent the system from forming products directly, and only the Π state allows the reaction to proceed. At near collinear geometry, the adiabatic ground state is attractive, but no potential energy well is present for the system to temporarily form a complex. The adiabatic excited state is correlated with the $OH(A^2\Sigma^+)$ + H; therefore, if the reaction starts on the excited state surface, a diabatic transition back to the ground state at some point is required for the reaction to occur.

On the ground state surface, classical and quasiclassical trajectory studies show that most of the reactions proceed through insertion geometry because of the deep potential minimum and the absence of a potential barrier in the entrance channel. This even applies to cases where the initial approach is collinear.[28] This is because the hydrogen molecule is so light that it can respond to any rapid change in the potential energy almost adiabatically and reorient itself so eventually the oxygen atom will be at the lateral position. Only a small portion of the reactions will go through the direct abstraction pathway without reorientation. Under most conditions, the complex will stay together and sample the potential

minimum several times before decomposing into products. Because the water complex acquires a lot of bending motion during the insertion process, the complex will invert several times through its linear geometry H-O-H before dissociating into products. The system therefore has time to redistribute its energy among different degrees of freedom and this is the reason why most theoretical studies on the ground state surface show a monatomic decrease in the vibrational state distribution of the OH product. This distribution resembles the *prior* distribution obtained from statistical theories. However, by tracking the time that the three atoms stay together, studies[24,26,28] show that the lifetime of the water complex is on the order of a few vibrational periods and less than a rotational period of a water molecule, so unimolecular decomposition theory is not applicable here. The same studies also show that for reactions that only go through the potential minimum once or do not go through it at all, the mechanism is direct and an inverted OH product vibrational distribution is observed. This inversion increases with the collisional energy and indicates the redistribution of the excess energy among different degrees of freedom is not complete. Most studies suggest the insertion process is more dominant than the direct abstraction pathway; therefore, they cannot explain the inverted vibrational energy distribution as observed in the experiments.

On the first excited state surface, there are only a few studies[28,29] carried out on the possible impact to this reaction. Since there is a significant barrier when the oxygen atom attacks the hydrogen molecule laterally on the first excited surface, only the collinear approach is important to our discussion. Calculation[32d]

suggests there is only a small barrier (~0.105 eV) for this approach. Therefore, it is possible it will contribute a significant amount to this system. As mentioned earlier, reactions starting on this surface must go through an avoided crossing and cross back to the ground adiabatic surface before the reaction can occur. This crossing, according to theoretical calculations,[29] occurs in the exit channel. Studies[28,29] show that most reactive encounters go directly to the products; only a small portion will fall back into the deep potential energy well (i.e. the H_2O minimum) and proceed just like the reactions starting on the ground state surface. One study[29] also suggests that some of the reactions on this surface will go through migration,[48] so the oxygen atom actually reacts with the second hydrogen atom instead of the first one it encounters. For those direct abstraction reactions, the OH products possess an excess amount of vibrational energy and show an inverted vibrational distribution. At the same time, the OH products are strongly backward scattered with respect to the incoming oxygen atoms. Such behavior is analogous to the findings of the $F + H_2$ reaction.

Based on the result from this experiment that a significant amount of the OH products scatter into the backward direction with respect to the $O(^1D)$ beam, it is suggested that the collinear approach of the oxygen atom to the hydrogen molecule plays a far more important role in this reaction than previously realized and so does the first excited state surface. This is in agreement with the fact that most of the calculations carried out on the ground state surface could not reproduce the inverted vibrational state distribution observed in the laboratory. Therefore it is more appropriate to include the first excited state in future studies

of this system. If indeed the first excited state surface is involved in this reaction, our result suggests that the entrance channel energy barrier on this surface should not be larger than the collisional energy used in this study, which is 2.3 kcal/mole. This agrees fairly well with the available theoretical value (~0.105 eV). Since early kinetic study[6] suggested that this reaction proceed essentially without any energy barrier, this barrier height could be even lower. The fact that we see a broad peak in the backward scattered direction in the OH product flux-velocity contour diagram also agrees with the theoretical predictions that the avoided crossing of the two adiabatic surfaces is energetically accessible within a large range of O-H-H bond angles.

The slight dip at the exact backward scattered position in our flux-velocity contour diagram is possibly due to the nonreactive events on the ground state surface from the strictly collinear approach. The origin of this nonreactivity has been discussed earlier. However, this strict collinear approach on the ground state surface does not preclude the system from going back to the deep potential well to form products through an insertion geometry.

It is well known for reactions like $F + H_2 \longrightarrow HF + H$ that when the collinear abstraction pathway is dominant, the product's rotational energy distribution is very cold; but in this case studies show that the OH products possess a large amount of rotational energy. Although it is possible that the collisional energy used in those investigations may be slightly below the energy barrier due to the thermalization of the $O(^1D)$ atoms before any reaction takes place, it is not a sufficient explanation since experiments under similar conditions

observed the inverted vibrational energy distribution. According to the theoretical study[29] on the first excited state surface, the OH product rotational distribution still strongly resembles the distribution obtained for the insertion process, only with a slight increase in the low j′ products. The authors attribute the high j′ products to the migration mechanism, which was originally proposed for alkali-metal halogen reactions.[48]

Another possible reason is the lack of constraint on the OH product rotational angular momentum despite the requirement of total angular momentum conservation. For reactions going through near collinear geometry, even if the initial total angular momentum may be small, the final rotational angular momentum of the OH product can still be quite large if it can be compensated by the final orbital angular momentum of the products in order to conserve the total angular momentum. In other words, if the rotational angular momentum of the OH product is pointing in the opposite direction of the final orbital angular momentum, the total angular momentum can still be conserved.

To demonstrate the validity of the above argument, let's assume the OH product is in the v′ = 2 and j′ = 18 state (we use v′ = 2 and j′ = 18 here since the vibrational distribution will be inverted for the collinear approach and j′ = 18 is the most populated rotational state in this vibrational state as found in the experiment[13]). The translational energy release is therefore around 10 kcal/mole, which translates into ~ 9400 m/s for the relative velocity between the two departing particles. We further assume that the initial total angular momentum is negligible, so we have

Final rotational angular momentum $\mathbf{J}' \approx$ *Final orbital angular momentum* $\mathbf{L}'$.

From the equation

Final orbital angular momentum $\mathbf{L}' = \mu\, \mathbf{v}\, \mathbf{b}$,

where μ is the reduced mass of the products, $\mathbf{v}$ is the relative velocity, and $\mathbf{b}$ is the impact parameter. We can then calculate the impact parameter for the product channel, which turns out to be ~ 1.3 Å. It is only slightly larger than the equilibrium distance of the OH molecule on the ground vibrational state and comparable to the impact parameters for the collinear approach that will lead to reaction. So, the constraint of total angular momentum conservation does not rule out the possibility of forming highly rotationally excited OH products.

Although a more backward peaked angular distribution was observed in this experiment, the insertion process is still believed to dominate the dynamics of this reaction. Most of the flat background in the OH product center-of-mass angular distribution should come from insertion. If the forward scattered peak is from the insertion process, due to the homonuclear nature of the hydrogen molecule, there should be an equal contribution in the backward scattered direction. However, the slow component does not show any obvious peaking in either direction. As mentioned in the 'RESULTS AND ANALYSIS' section, the only possible way to fit the results with a symmetric and an asymmetric component is to assume an isotropic or sideways peaked angular distribution for the symmetric case. This agrees with some theoretical studies[22] where angular distributions other than forward and backward peaked are obtained. If the migration mechanism does play a role in this reaction, this process will contribute mainly to the forward scattered

peak in the angular distribution and therefore it can explain the existence of the forward scattered peak. Thus, it is uncertain if the insertion process will in fact produce a forward and backward peaked center-of-mass angular distribution as most studies have suggested.

It was brought to our attention that, in parallel with this work, Casavecchia's group in Italy also carried out the crossed molecular beams experiment on the same system using two continuous beam sources.[49] Detailed studies was performed at collisional energies of 3 and 4 kcal/mole, respectively. Because of their very precise measurements, a faint structure was observed in the OH product laboratory angular distribution, near the center-of-mass and at wide angles. By using six sets of $P(E_t)$s and $T(\Theta)$s to account for all the energetically accessible OH vibrational states, the vibrational energy distribution was able to be determined. At 4 kcal/mole collisional energy, the vibrational distribution is peaked at $v' = 3$, with slightly less but equal population in the lower vibrational states. Their center-of-mass angular distributions favor backward scattered direction at low v' states ($v' = 0$ and 1), but become more forward scattered at high v' states ($v' = 2 - 4$). Even though their collisional energies are higher than the one used in this study, results obtained in their study seems to corroborate with our findings. At higher translational energy releases (low v' states) the products are backward scattered, and at lower translational energy (mixings of low and high v' states) the distribution starts to become more symmetric with respect to 90°.

At last, it is necessary to point out that the above discussion is entirely limited to singlet surfaces. However, there is evidence that to a small extent triplet

surfaces are also involved in this reaction. By measuring the Λ-doublet components of the OH products at high rotational states (Λ-doublet is only well defined at high rotational states),[13,18] it was found that the Π^+ component is strongly dominant over the Π^- component. The Π^+ component corresponds to the singly occupied Π orbital lying on the rotating plane of the OH molecule and the Π^- component corresponds to a perpendicular orientation. Since in this case the three atoms form a unique plane, intuitively following the dissociation, the rotation of the OH molecule will remain on this plane and so will be the unpaired electron. Therefore, the dominance of the Π^+ component is expected. The fact that people observed the Π^- component suggests that a triplet surface is also involved in this reaction by spin-orbit interaction. This interaction can be explained by the crossing of the two surfaces ($^1A'$ in $O(^1D) + H_2$ and $^3A''$ in $O(^3P) + H_2$ surfaces) at the entrance channel.[19,32a] This spin forbidden crossing generates more rotationally cold OH molecules and is not considered to be important in this reaction since the observed OH rotational distribution is highly inverted. However, studies[18] on reactions between $O(^1D)$ atoms and large hydrocarbons such as C_2H_6 and $C(CH_3)_4$ have shown it contributes significantly, and the resulting OH rotational state distribution is bimodal.

CONCLUSIONS

We have reinvestigated the reactions between $O(^1D)$ atoms and H_2 molecules using the crossed molecular beams technique with two pulsed beams. The time resolution was improved over the previous study in order to resolve any possible vibrational structure. Even though this structure was not resolvable due to the broad and inverted distribution of the OH rotation, the OH product center-of-mass flux-velocity contour map showed more backward scattered intensity in contrast to previous findings. Our results, along with results from theoretical calculations, suggest the possible involvement of the first excited state energy surface in this reaction. On this surface, the collinear approach dominates; after the system jumps back to the ground state surface, the OH products are formed favoring the backward scattered direction with respect to the oxygen atom beam. The energy barrier for the collinear approach on this surface should be comparable to or lower than the collisional energy used in this experiment. The involvement of the first excited state surface also produces more vibrationally excited OH products, which can explain the inverted vibrational structure observed in the LIF and other experiments. This study should provide ground work for future theoretical studies on this reaction to include the first excited state potential energy surface.

Because of the uncertainties in some regions of the time-of-flight spectra and the laboratory angular distribution near the center of mass of this system,

further attempt to separate the products into symmetric and asymmetric center-of-mass angular distributions was not made. To reduce the errors in the result and to improve our counting statistics, a different precursor for the $O(^1D)$ beam such as N_2O may be more suitable in the future.

Preliminary studies on the $O(^1D)$ + HD reaction were also carried out with hopes of determining the isotopic branching ratio of this reaction. However, due to the kinematics of this reaction and the high m/e = 18 background count rate in our detector, the OD product was very hard to detect and so the results were not reported here.

With the successful operation of the pulsed $O(^1D)$ atom beam, there are now many other reactions that can be studied. In particular, reactions between $O(^1D)$ atoms and N_2O, CO_2, H_2O and hydrocarbons are very important processes in atmospheric chemistry. In the meantime, we should also be able to apply the same photolytic technique to produce other beam sources, such as OH radicals, to study a wealth of different reactions.

APPENDIX A

This appendix will briefly discuss the effect of the nozzle-to-skimmer distance on the quality of pulsed nozzle beams. For a continuous molecular beam source, even if there is interaction between the beam and the skimmer, this interaction will alter the beam quality in the same way at every point in time. On the other hand, because the pulsed nozzle beam is not continuous, this interaction becomes time dependent. In addition, since the intensity of the pulsed beam is typically one or two orders of magnitude higher than that of a continuous beam, the interaction is usually more severe so extra attention is required.

To illustrate the effect of this interaction and the way the optimum nozzle-to-skimmer distances were determined for this experiment, the following procedure was carried out. As the nozzle-to-skimmer distance was varied, the change of the pure He beam intensity within the pulse was recorded. A mechanical chopper was used to sample the beam in front of the skimmer and the photodiode signal originating from the chopper served as the time reference. To obtain the beam intensity at each time delay, the pulsed valve delay with respect to the mechanical chopper trigger signal was changed, time-of-flight spectra were recorded and the peak in each spectrum was integrated. Spectra taken at longer time delays represented the earlier part of the pulse and vice versa. Fig. A-1 shows the He beam profiles at six different nozzle-to-skimmer distances (d). As shown in this figure, when the skimmer is very close to the pulsed nozzle ($\leq$10

mm), the interaction of the front part of the pulse with the skimmer is so strong that when the beam reaches the middle part of the pulse, the pressure buildup in front of the skimmer starts to interfere with the beam and this part of the pulse is greatly attenuated. As one might expect, the onset of the interaction happens earlier when the nozzle is moved closer to the skimmer and the attenuation becomes more pronounced. Eventually the beam will be completely destroyed. As the nozzle is moved away from the skimmer, the interaction becomes less significant and the smooth, single peaked pulsed beam profile is observed. If the nozzle continues to be moved farther away from the skimmer, even though the beam profile remains the same, the beam intensity begins to drop gradually (d = 20 mm). The same behavior was also observed for the ozone beam used in the production of $O(^1D)$ atom beams when the nozzle was placed too close to the skimmer. Fig. A-2 shows the temporal profile of the ozone beam ($\approx$ 1% O_3 seeded in helium) at d = 10 mm the ozone beam velocity and its speed ratio distributions within the pulse. Although the beam velocity within the pulse is expected to gradually decrease due to the nature of the pulsed beam, it is clearly seen that the interaction induces more drop in the beam velocity around 80~90 μsec and not until the later part of the pulse does the beam regain its velocity. Therefore, a larger nozzle-to-skimmer distance (d = 12 mm) was chosen for the $O(^1D) + H_2$ experiment. Surprisingly, the speed ratio of the ozone beam does not change considerably during the interaction.

From the above experiment, it is clear that the interaction between the pulsed beam and the skimmer has a significant impact on the beam quality if the

nozzle-to-skimmer distance is not chosen properly. This especially affects the middle part of the pulse. The effect on the beginning and the tail of the pulse is not so severe, but usually those parts of the pulse are either too unstable or too weak for practical use. Therefore, determination of the nozzle-to-skimmer distance is extremely important in a pulsed molecular beam experiment.

APPENDIX B

Since in this experiment the differential pumping regions for both sources were omitted in order to adapt to the pulsed valves and the introduction of the photolyzing laser, molecules diffusing out of the source region into the collision chamber occurred more often, and therefore background scattering became an important issue. In an earlier attempt of this experiment, some unrealistic features appeared up in the OH product time-of-flight spectra and also in its laboratory angular distribution. In this appendix, it will be shown how background scattering can affect the experimental results and how to overcome this difficulty.

To illustrate the problem raised by background scattering, a Ne + He elastic scattering experiment was performed with variable delays between the two pulses. The setup was the same as the one used in the $O(^1D) + H_2$ experiment, except the $O(^1D)$ and H_2 beams were replaced by the pure Ne and He beams, respectively. In addition, the photolyzing laser was not used. The chopped Ne beam was about 8 μsec in duration. Fig. B-1 shows the attenuation of the Ne beam due to the interaction with the He gas pulse at different time delays. Since the attenuation curve should reflect the profile of the He beam, it suggests that the He beam has a great deal of interaction with the skimmer. Fig. B-2 shows the Ne time-of-flight spectra at several different delays at 12.5°. Note that with a longer He pulsed beam delay, the earlier part of the He pulse will intersect with the chopped Ne beam. As shown in this figure, a spurious peak starts to appear in the spectra and

becomes more pronounced as the delay becomes shorter. Since the attenuation of the Ne beam is limited to about 15% or less, it is unlikely this peak comes from multiple scattering events, therefore scattering with the background molecules is responsible for this artifact. At the beginning of the He pulse, since the source chamber pressure is still low, the diffusive background coming out of the source is not significant. After the pressure has built up in the source, the diffusive background cannot be neglected anymore.

The background scattering also contributed significantly in the $O(^1D) + H_2$ experiment. Fig. B-3 shows the OH product laboratory angular distribution obtained in an earlier attempt of this reaction. In that experiment, the timing between the two beam pulses was chosen such that the $O(^1D)$ beam overlapped with the middle part of H_2 pulses and the resulting OH product laboratory angular distribution showed a continuous rising near the $O(^1D)$ beam. It was then found that this unrealistic feature was dependent upon the timing of the two pulses. As a result, a longer time delay was eventually used. By doing so, the beam intensities, and possibly the quality of the beams, were inevitably sacrificed. This is a tradeoff that has to be taken into consideration when designing a crossed beams experiment using two pulsed beams.

REFERENCES

1. J. R. Wiesenfeld, Acc. Chem. Res. **15**, 110 (1982).
2. D. M. Neumark, A. M. Wodtke, G. N. Robinson, C. C. Hayden, and Y. T. Lee, J. Chem. Phys. **82**, 3045 (1985).
3. A. B. Callear and H. E. van den Bergh, Chem. Phys. Lett. **8**, 17 (1971).
4. Y. Huang, Y. Gu, C. Liu, X. Yang, and Y. Tao, Chem. Phys. Lett. **127**, 432 (1986).
5. J. Shao, L. Yuan, H. Yang, Y. Gu, K. Li, K. Wang, and Y. Tao, XIVth International Symposium on Molecular Beams, LBL report 32305 (1992).
6. W. B. DeMore, J. Chem. Phys. **47**, 2777 (1967).
7. J. A. Davidson, C. M. Sadowski, H. I. Schiff, G. E. Streit, C. J. Howard, D. A. Jennings, and A. L. Schmeltekopf, J. Chem. Phys. **64**, 57 (1976).
8. A. C. Luntz, R. Schinke, W. A. Lester, Jr., and Hs. H. Günthard, J. Chem. Phys. **70**, 5908 (1979).
9. G. K. Smith, J. E. Butler, and M. C. Lin, Chem. Phys. Lett. **65**, 115 (1979).
10. G. K. Smith and J. E. Butler, J. Chem. Phys. **73**, 2243 (1980).
11. G. M. Jursich and J. R. Wiesenfeld, Chem. Phys. Lett. **119**, 511 (1985).
12. J. E. Butler, G. M. Jursich, I. A. Watson, and J. R. Wiesenfeld, J. Chem. Phys. **84**, 5365 (1986).
13. C. B. Cleveland, G. M. Jursich, M. Trolier, and J. R. Wiesenfeld, J. Chem. Phys. **86**, 3253 (1987).

14. J. E. Butler, R. G. Macdonald, D. J. Donaldson, and J. J. Sloan, Chem. Phys. Lett. **95**, 183 (1983).

15. P. M. Aker and J. J. Sloan, J. Chem. Phys. **85**, 1412 (1986).

16. K. Tsukiyama, B. Katz, and R. Bersohn, J. Chem. Phys. **83**, 2889 (1985).

17. R. J. Buss, P. Casavecchia, T. Hirooka, S. J. Sibener, and Y. T. Lee, Chem. Phys. Lett. **82**, 386 (1981).

18. A. C. Luntz, J. Chem. Phys. **73**, 1143 (1980).

19. Y. Matsumi, K. Tonokura, Y. Inagaki, and M. Kawasaki, J. Phys. Chem. **97**, 6816 (1993).

20. The H/D ratio obtained in Ref. 16 has been constantly misinterpreted. Readers have to pay great attention to those papers that quoted this number. For example, Ref. 12 quoted this number correctly, but misinterpreted their own results. Both Ref. 13 and Ref. 24 misquoted this number and claimed this reaction should produce more OH than OD products.

21. K. S. Sorbie and J. N. Murrell, Mol. Phys. **31**, 905 (1976).

22. R. Schinke and W. A. Lester, Jr., J. Chem. Phys. **72**, 3754 (1980).

23. S. W. Ransome and J. S. Wright, J. Chem. Phys. **77**, 6346 (1982).

24. P. A. Whitlock, J. T. Muckerman, and E. R. Fisher, J. Chem. Phys. **76**, 4468 (1982).

25. L. J. Dunne and J. N. Murrell, Mol. Phys. **50**, 635 (1983).

26. P. A. Whitlock, J. T. Muckerman, and P. M. Kroger, in *Potential Energy Surfaces and Dynamics Calculations*, edited by D. G. Truhlar (Plenum, New York, 1981), p551.

27. P. A. Berg, J. J. Sloan, and P. J. Kuntz, J. Chem. Phys. **95**, 8038 (1991).

28. P. J. Kuntz, B. I. Niefer, and J. J. Sloan, Chem. Phys. **151**, 77 (1991).

29. P. J. Kuntz, B. I. Niefer, and J. J. Sloan, J. Chem. Phys. **88**, 3629 (1988).

30. J. K. Badenhoop, H. Koizumi, and G. C. Schatz, J. Chem. Phys. **91**, 142 (1989).

31. M. S. Fitzcharles and G. C. Schatz, J. Phys. Chem. **90**, 3634 (1986).

32. There are many potential energy surface calculations available for this system, therefore only a few important ones will be given here. (a) R. E. Howard, A. D. McLean, and W. A. Lester, Jr., J. Chem. Phys. **71**, 2412 (1979). (b) G. Durand and X. Chapuisat, Chem. Phys. **96**, 381 (1985). (c) J. N. Murrell and S. Carter, J. Phys. Chem. **88**, 4887 (1984). (d) S. P. Walch and L. B. Harding, J. Chem. Phys. **88**, 7653 (1988).

33. K. Rynefors, P. A. Elofson, and L. Holmlid, Chem. Phys. **100**, 53 (1985).

34. P. A. Elofson, K. Rynefors, and L. Holmlid, Chem. Phys. **100**, 39 (1985).

35. R. D. Levine and R. B. Bernstein, Chem. Phys. Lett. **29**, 1 (1974).

36. R. B. Bernstein, Int. J. Quan. Chem. Symp. **9**, 385 (1975).

37. Y. T. Lee, J. D. McDonald, P. R. LeBreton, and D. R. Herschbach, Rev. Sci. Instrum. **40**, 1402 (1969).

38. R. E. Continetti, Ph. D. Thesis, University of California, Berkeley (1989).

39. R. K. Sparks, L. R. Carlson, K. Shobatake, M. L. Kowalczyk, and Y. T. Lee, J. Chem. Phys. **72**, 1401 (1980).

40. S. T. Amimoto, A. P. Force, J. R. Wiesenfeld, and R. H. Young, J. Chem. Phys. **73**, 1244 (1980).

41. D. Proch and T. Trickl, Rev. Sci. Inst. **60**, 713 (1989).

42. a) N. F. Daly, Rev. Sci. Inst. **31**, 264 (1960).

b) H. M. Gibbs and E. D. Commins, Rev. Sci. Inst. **37**, 1385 (1966).

43. a) M. F. Vernon, Ph. D. Thesis, University of California, Berkeley (1983).

b) D. J. Krajnovich, Ph. D. Thesis, University of California, Berkeley (1983).

44. H. Haberland, U. Buck, and M. Tolle, Rev. Sci. Inst. **56**, 1712 (1985).

45. R. Buss, Ph. D. Thesis, University of California, Berkeley (1979).

46. Even though the fast component accounts for 90% of the reactions taking place, due to the transformation between the center-of-mass frame and the laboratory frame, more products with slow velocities are actually observed. So 90% does not mean that the fast component accounts for 90% of the signals observed in this experiment.

47. For a more detailed correlation diagram, see S. Tsurubuchi, Chem. Phys. **10**, 335 (1975).

48. P. J. Kuntz, M. H. Mok, and J. C. Polanyi, J. Chem. Phys. **50**, 4623 (1969).

49. P. Casavecchia, private communication.

FIGURE CAPTIONS

Figure 1 Schematic view of the crossed molecular beam apparatus and the experimental setup. Note that it is not drawn to scale.

A - Pulsed $O(^1D)$ beam source;

B - Pulse H_2 beam source;

C - Photolyzing laser;

D - Chopper wheel;

E - Quadrupole mass spectrometer.

Figure 2 Timing relationships between the triggers used in this experiment and their typical values. The chopper is spun at 200 Hz with four opening slots, so the photodiode signal from the chopper wheel is 800 Hz. All delays are already corrected for the wheel offset.

Figure 3 The O^{2+} TOF spectra taken on axis of the ozone beam (0 degree).

(a) Circles : Laser on signal. Dotted line : Laser off signal.

(b) The subtracted O^{2+} signal. It took into account the amount of ozone depletion following dissociation (in this case 27.6%). The solid line is the fit assuming a supersonic beam velocity distribution.

Figure 4 Newton diagram for the reaction $O(^1D) + H_2 \longrightarrow OH + H$.

$O(^1D)$ beam velocity : 1900 m/s.

H_2 beam velocity : 2700 m/s.

Solid circle : the absolute maximum center-of-mass velocity for the OH product ($v' = 0$).

Dashed circles : the maximum center-of-mass velocities for the OH product in different vibrational states except $v' = 0$.

Figure 5 The OH product time-of-flight spectra before subtraction at six laboratory angles.

Circles : laser on signal.

Dotted lines : laser off signal.

Figure 6 The OH product laboratory angular distribution.

Filled circles : experimental results.

Solid line : the fit using the $P(E_t)$s and $T(\Theta)$s shown in Fig. 8 and Fig. 9.

Dotted line : the fit using the $P(E_t)$ and $T(\Theta)$ from Ref. 17.

Figure 7 The OH product time-of-flight spectra after subtraction and their corresponding fit using the $P(E_t)$s and $T(\Theta)$s shown in Fig. 8 and Fig. 9.

Figure 8 (a) The translational energy release distribution $P(E_t)$ for the fast component.

(b) Corresponding center-of-mass angular distribution $T(\Theta)$ for the fast component.

Figure 9 (a) The translational energy release distribution $P(E_t)$ for the slow component.

(b) Corresponding center-of-mass angular distribution $T(\Theta)$ for the slow component.

Figure 10 The OH product flux-velocity contour diagram constructed from the $P(E_t)$s and corresponding $T(\Theta)$s in Fig. 8 and Fig. 9. The outermost circle represents the maximum velocity the OH products can reach in this study. Also note that the $O(^1D)$ and H_2 center-of-mass velocities are not drawn to scale.

Figure 11 Energy level correlation diagram for the $O(^1D,^3P) + H_2$ system for several low lying states. Some energy levels are not drawn because they are not related to the discussion. It is only qualitative in nature. Several energy levels are shifted (e.g. $^1\Pi_u$ and $^3\Pi_u$) in order to present a clearer picture.

Figure A-1 Pulsed He beam profiles at several nozzle-to-skimmer distances (d). For clarity, they are separated into two figures.

Filled circles : d = 6 mm;

Filled triangles : d = 8 mm;

Filled squares : d = 10 mm;

Open circles : d = 12 mm;

Open triangles : d = 14 mm;

Open squares : d = 20 mm.

Figure A-2 Pulsed ozone beam profile at d = 10 mm and its corresponding velocity and speed ratio distributions.

Figure B-1 Attenuation curve of the Ne beam as a function of the pulsed He beam delay. The solid line is the spline fit. It is drawn for visual aid only.

Figure B-2 Time-of-flight spectra of the scattered Ne atoms at 12.5° at four different He beam delays.

Figure B-3 The distorted OH product laboratory angular distribution. The rising of the OH product intensities near the $O(^1D)$ beam is attributed to background scattering events.

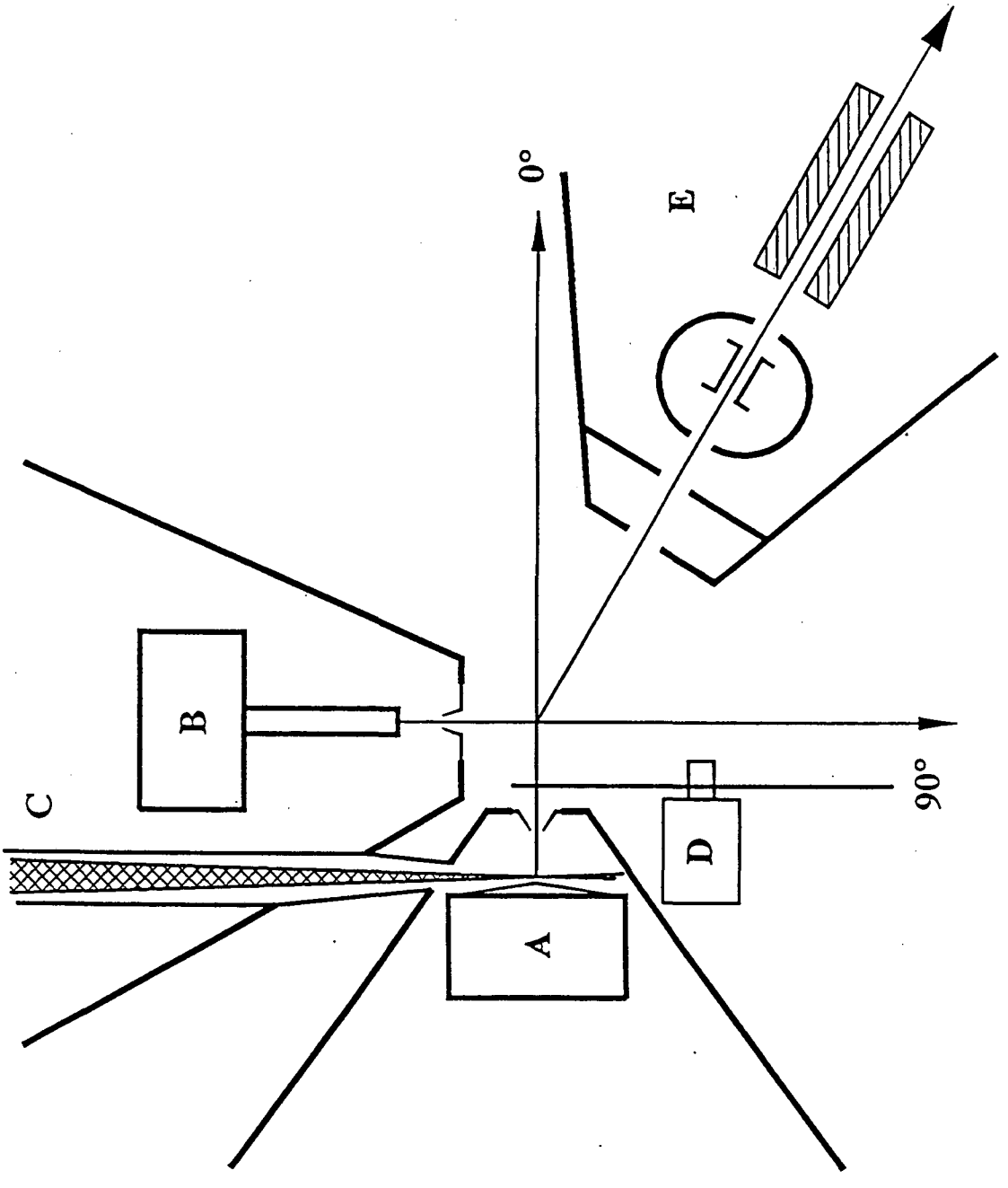

Figure 1

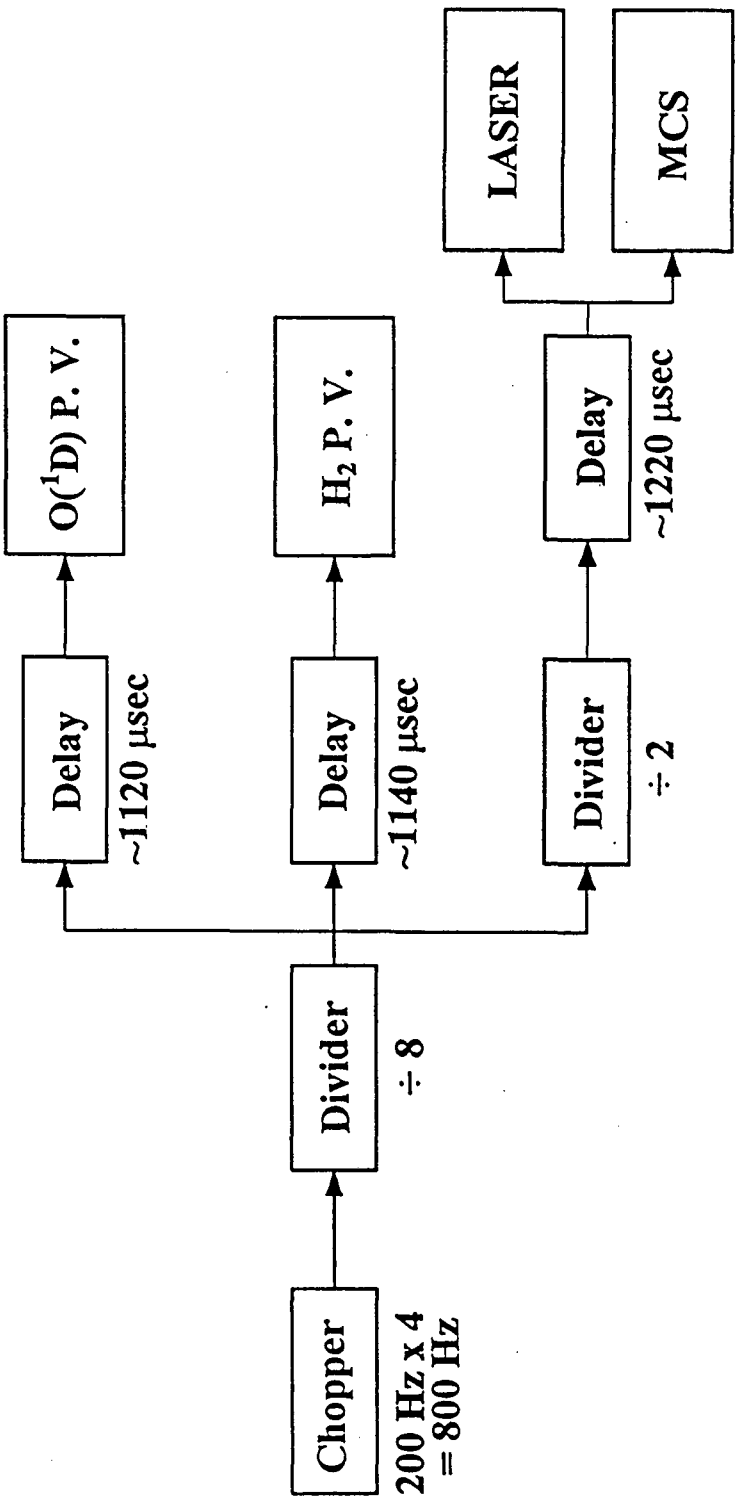
Chopper
200 Hz x 4
= 800 Hz
Divider
÷ 8
Delay
~1120 µsec
Delay
~1140 µsec
Divider
÷ 2
Delay
~1220 µsec
O(1D) P. V.
H2 P. V.
LASER
MCS

Figure 2

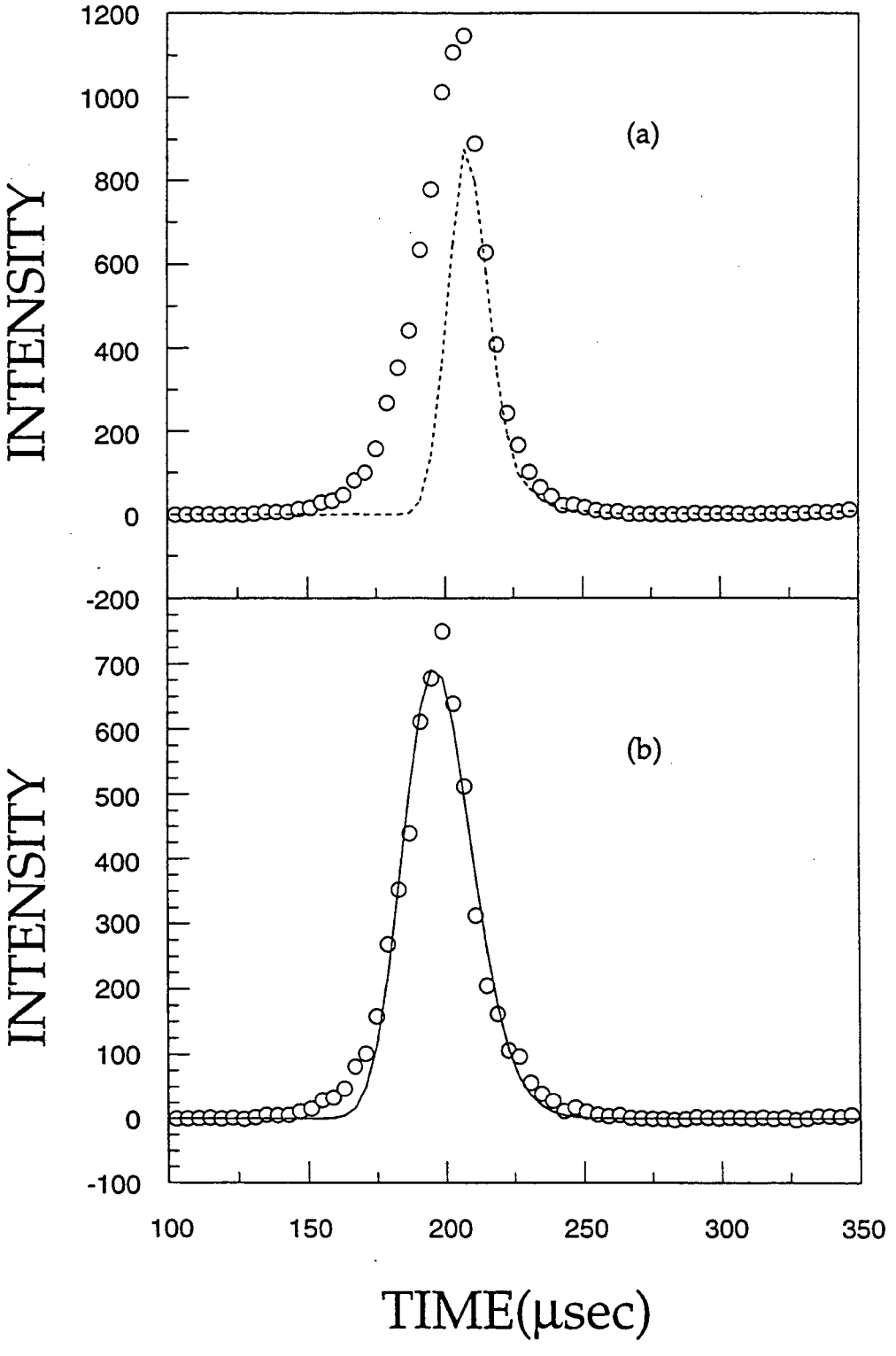
1200
1000
800
600
400
200
0
-200
INTENSITY
(a)
700
600
500
400
300
200
100
0
-100
INTENSITY
(b)
100
150
200
250
300
350
TIME(μsec)

Figure 3

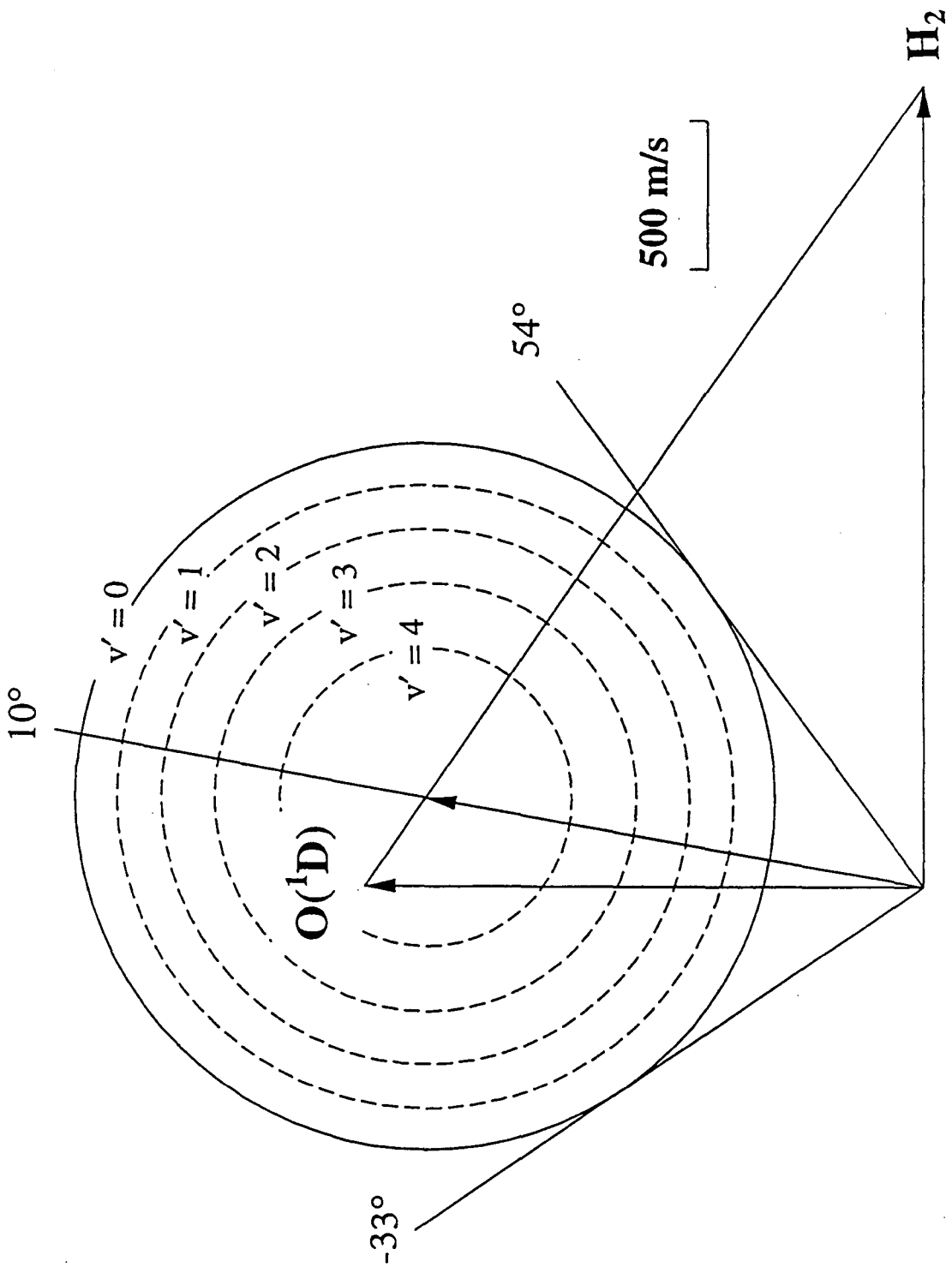

Figure 4

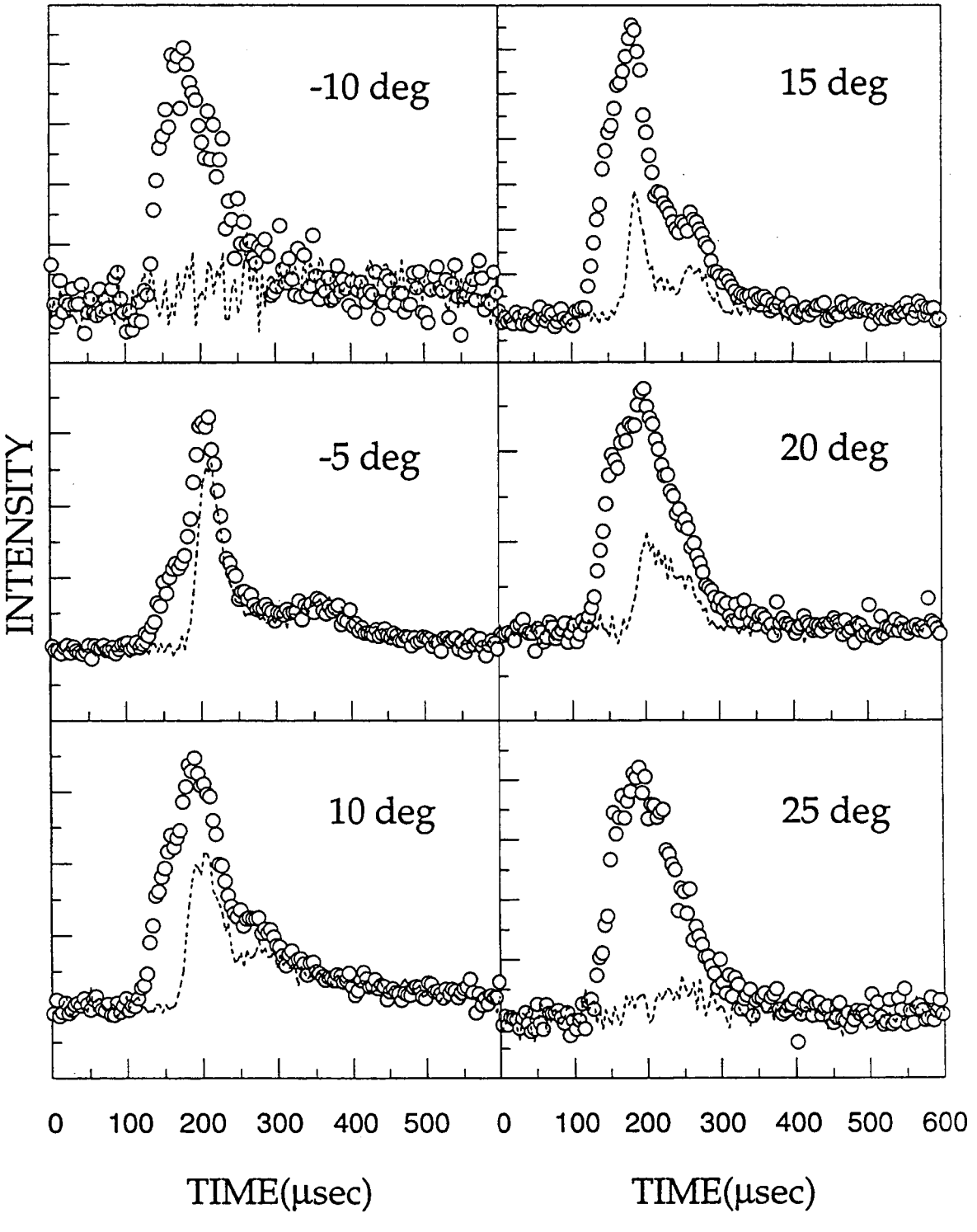
-10 deg
15 deg
-5 deg
20 deg
10 deg
25 deg
INTENSITY
0
100
200
300
400
500
0
100
200
300
400
500
600
TIME(μsec)
TIME(μsec)

Figure 5

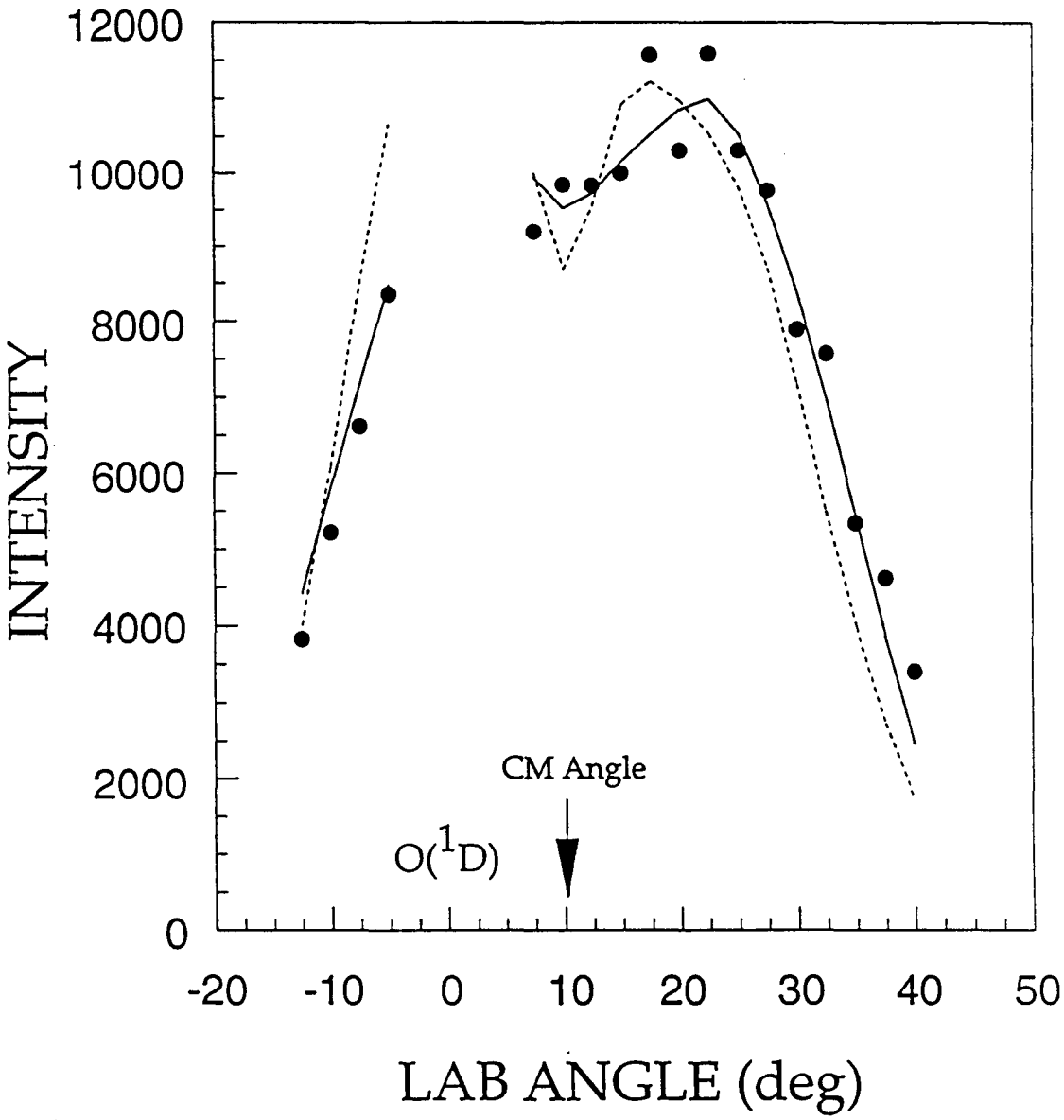
12000
10000
8000
6000
4000
2000
0
INTENSITY
CM Angle
O(1D)
-20
-10
0
10
20
30
40
50
LAB ANGLE (deg)

Figure 6

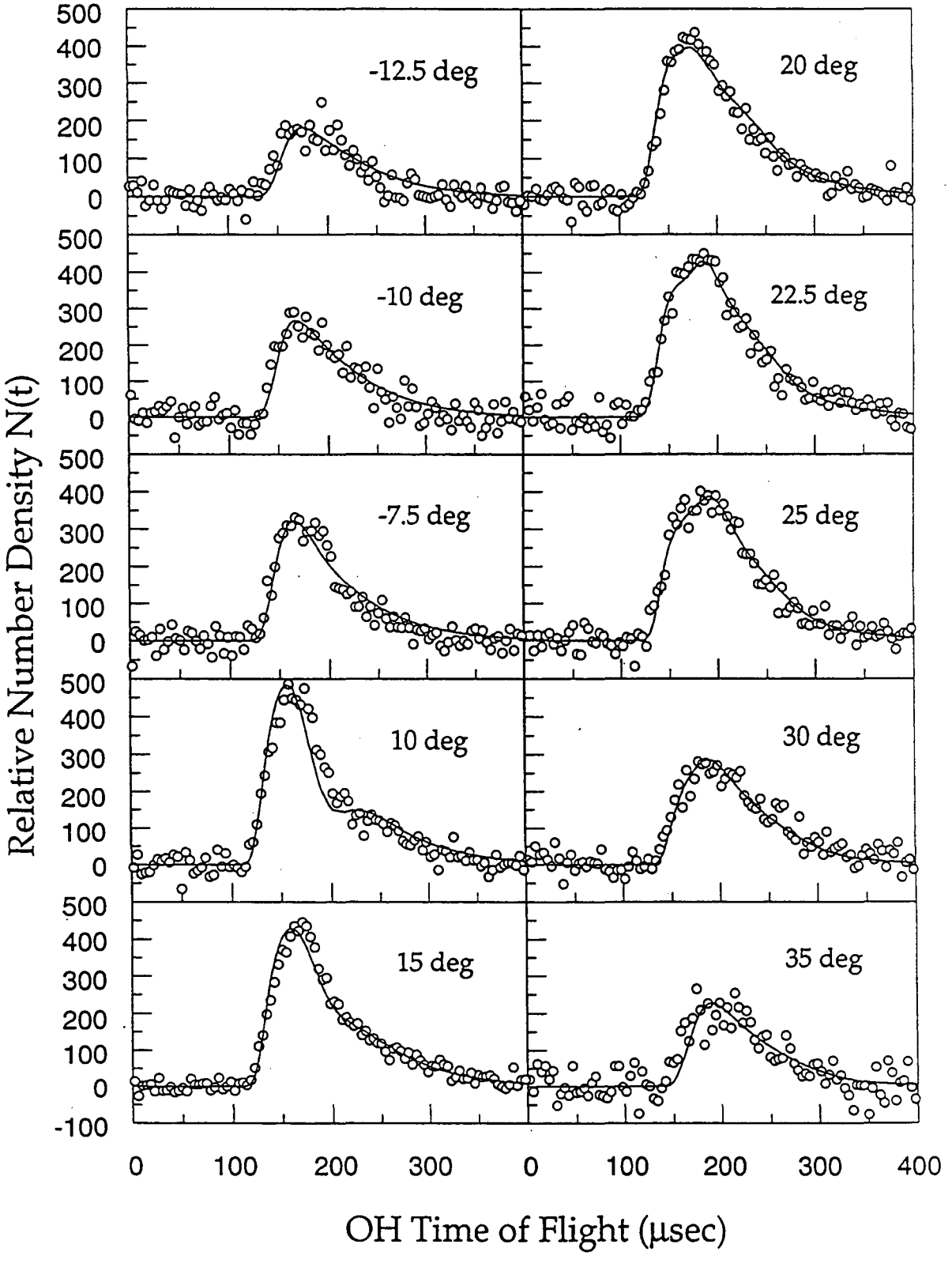
-12.5 deg
20 deg
-10 deg
22.5 deg
-7.5 deg
25 deg
10 deg
30 deg
15 deg
35 deg
Relative Number Density N(t)
OH Time of Flight (μsec)
500
400
300
200
100
0
-100
0
100
200
300
400

Figure 7

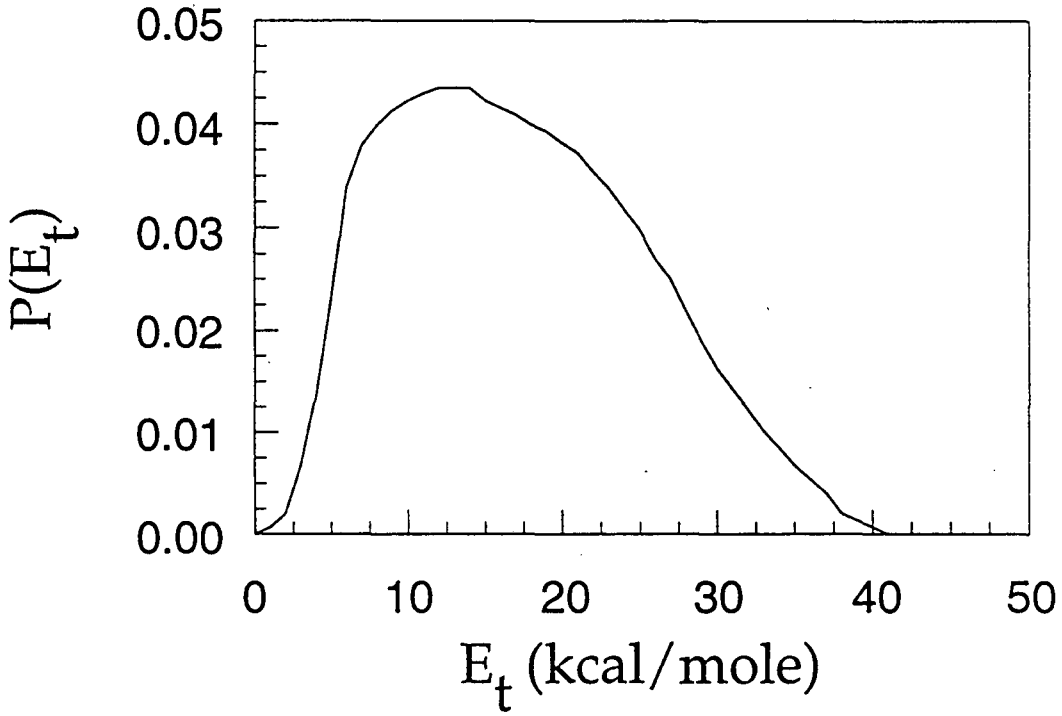
0.05
0.04
0.03
0.02
0.01
0.00
P(E_t)
0
10
20
30
40
50
E_t (kcal/mole)

(a)

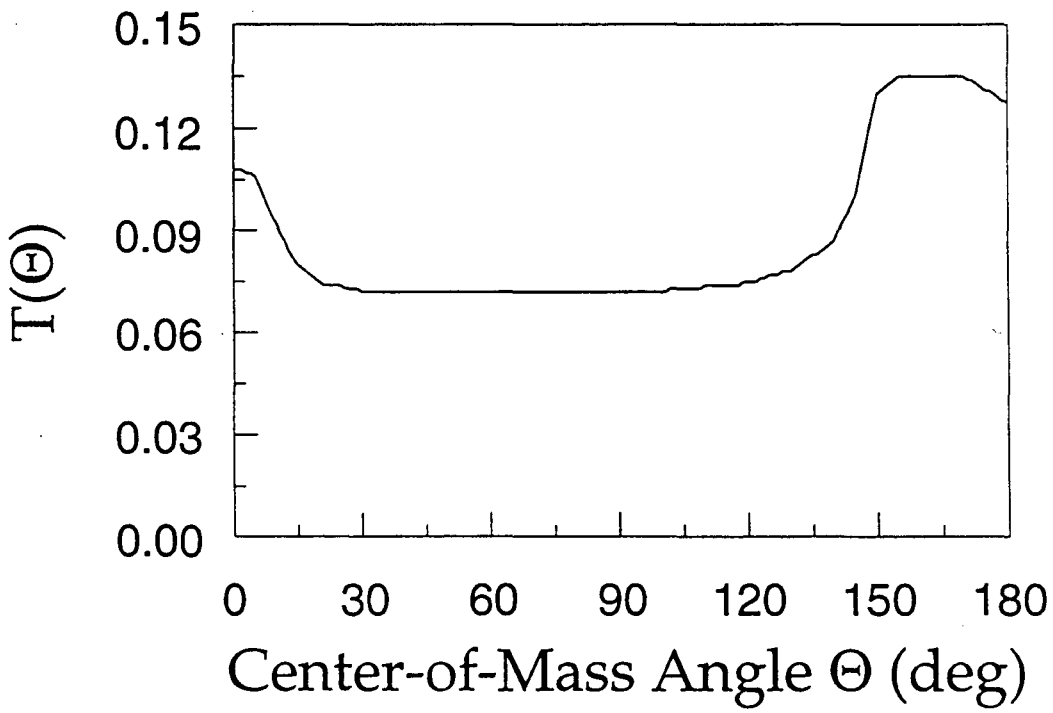
0.15
0.12
0.09
0.06
0.03
0.00
T(Θ)
0
30
60
90
120
150
180
Center-of-Mass Angle Θ (deg)

(b)

Figure 8

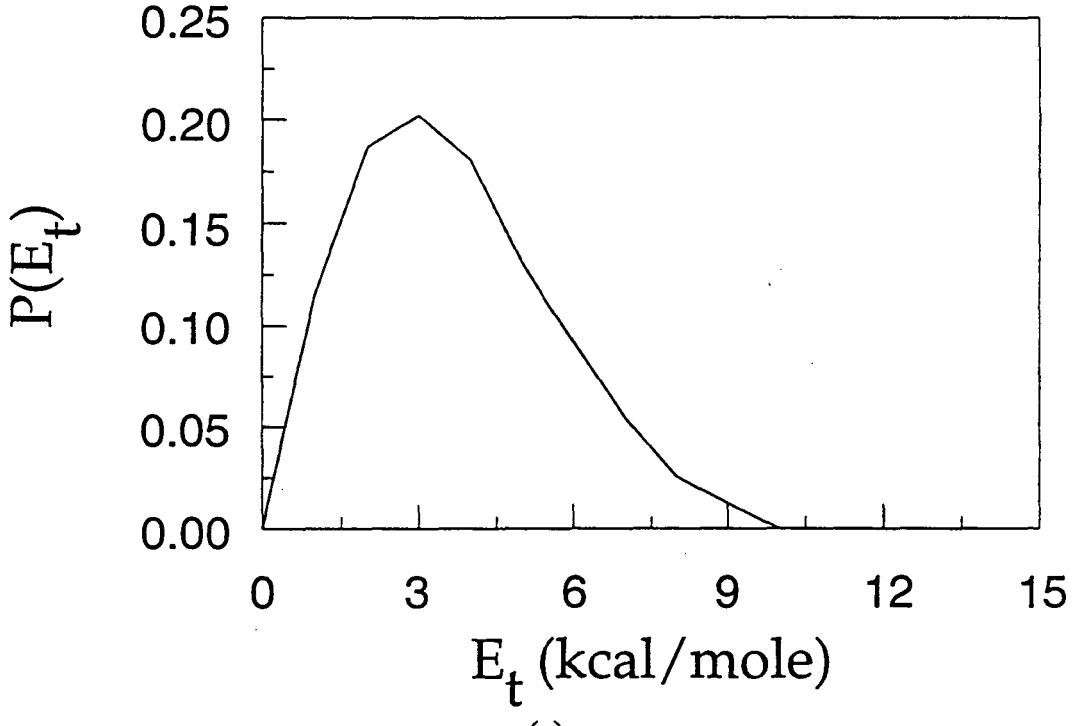
0.25
0.20
0.15
0.10
0.05
0.00
P(E_t)
0
3
6
9
12
15
E_t (kcal/mole)

(a)

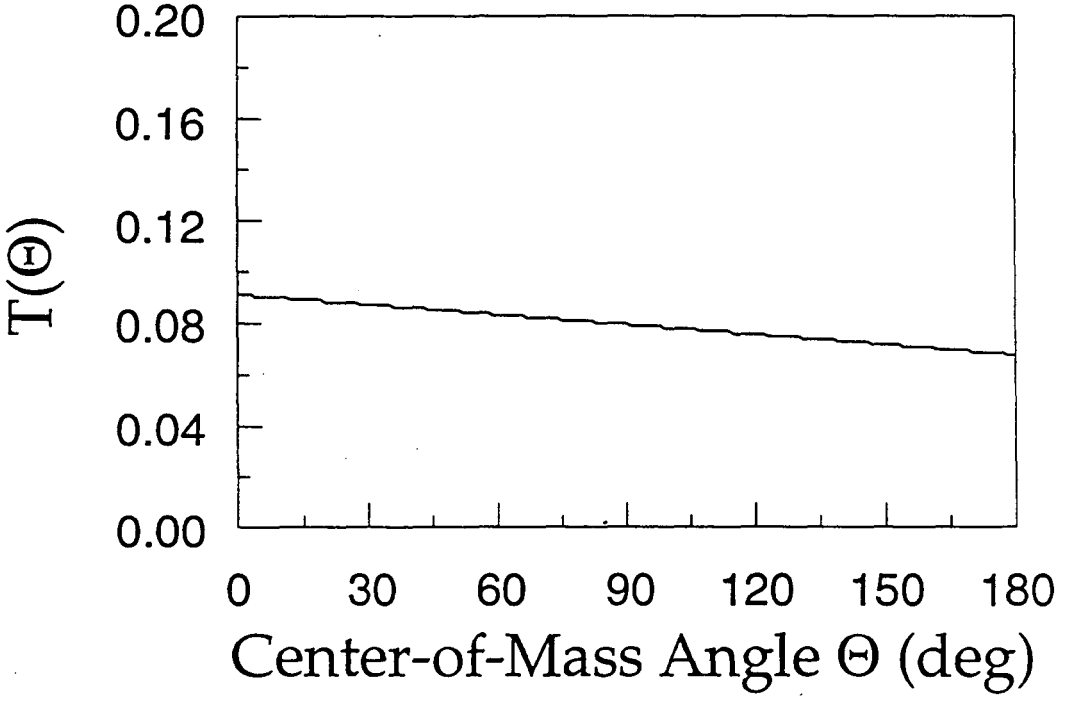
0.20
0.16
0.12
0.08
0.04
0.00
T(Θ)
0
30
60
90
120
150
180
Center-of-Mass Angle Θ (deg)

(b)

Figure 9

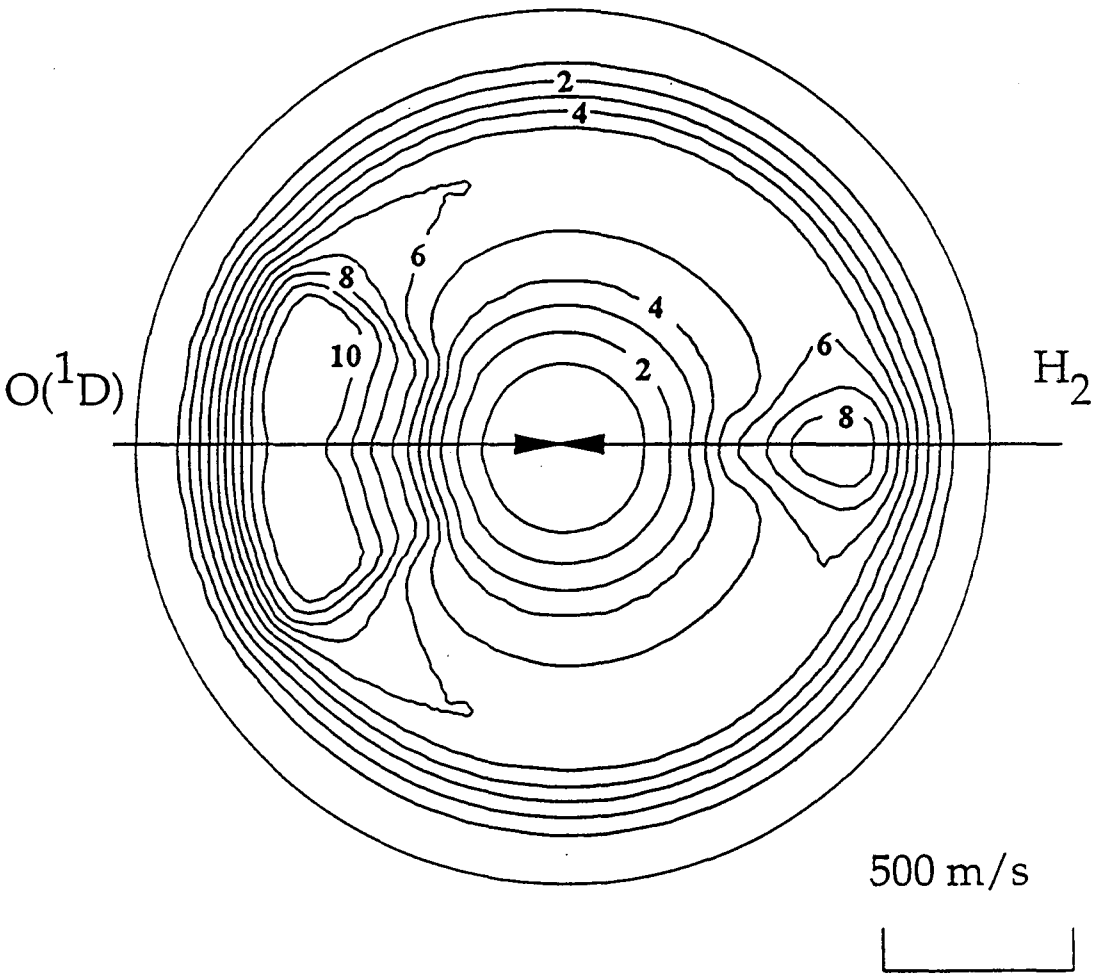

Figure 10

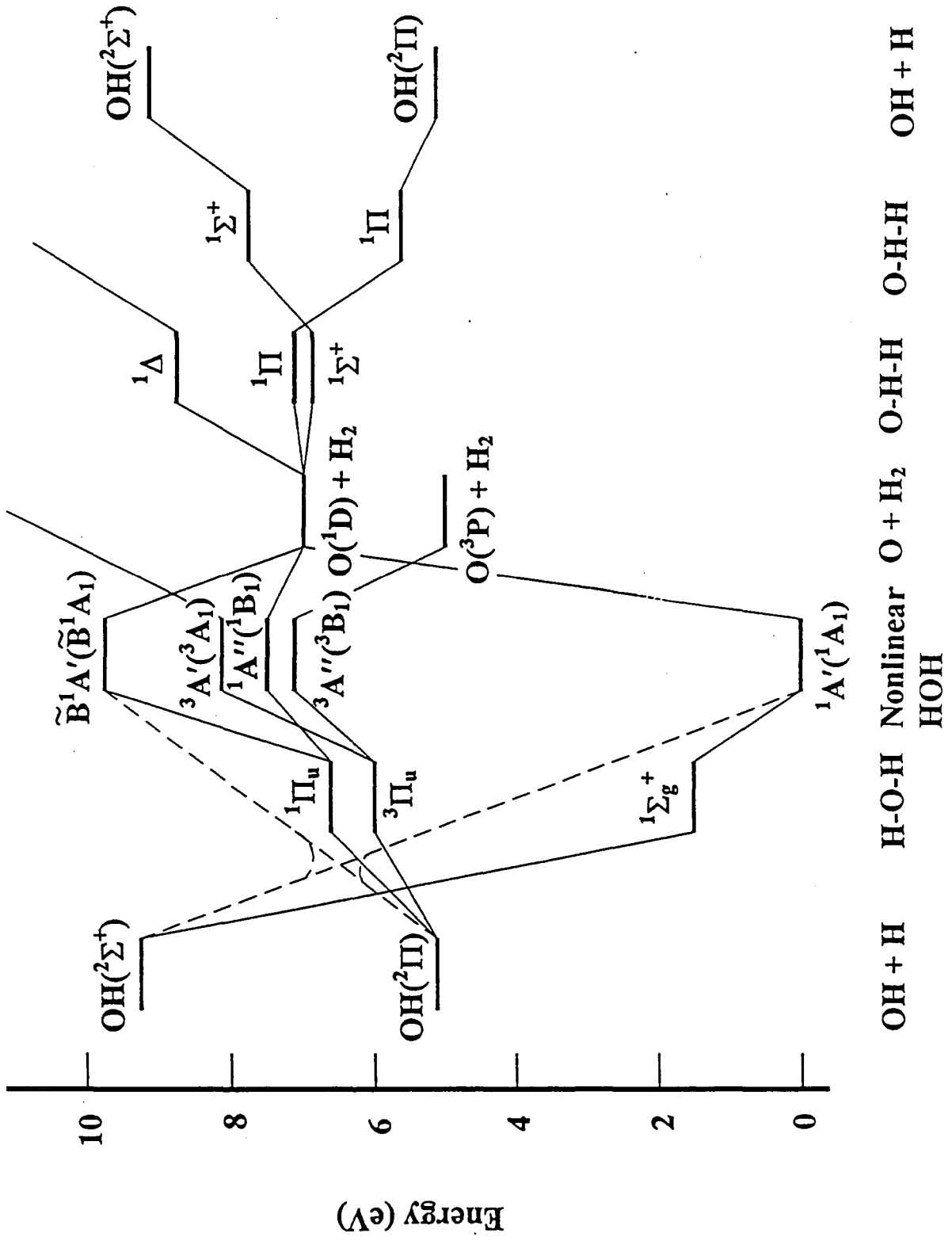
Energy (eV)
10
8
6
4
2
0
OH + H
H-O-H
Nonlinear
HOH
O + H2
O-H-H
O-H-H
OH + H
OH(2Σ+)
OH(2Π)
B̃1A′(B̃1A1)
3A′(3A1)
1A″(1B1)
3A″(3B1)
O(1D) + H2
O(3P) + H2
1Δ
1Σ+
1Π
1Π
1Σ+
1Π
OH(2Σ+)
OH(2Π)
1Πu
3Πu
1Σg+
1A′(1A1)

Figure 11

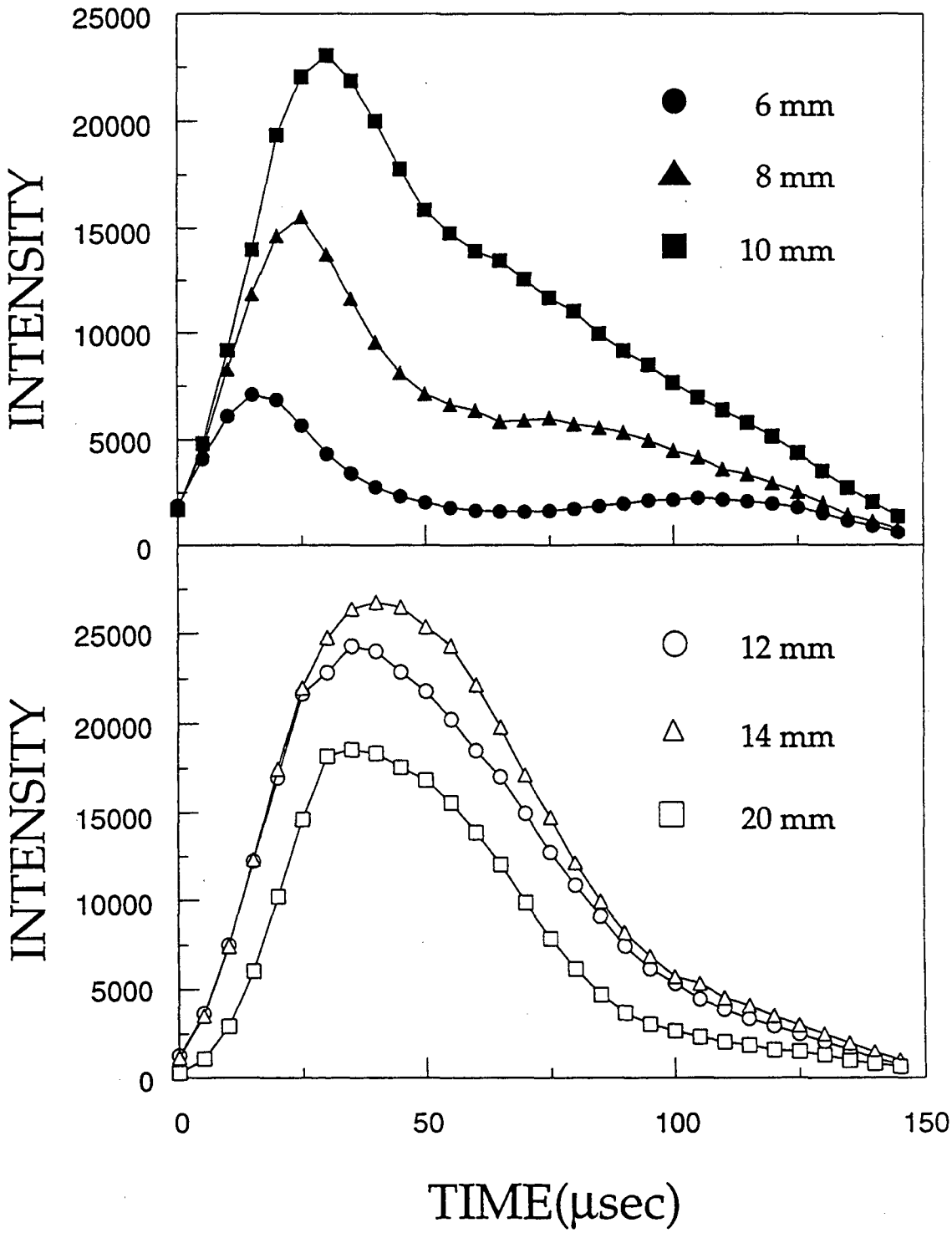
INTENSITY
25000
20000
15000
10000
5000
0
6 mm
8 mm
10 mm
INTENSITY
25000
20000
15000
10000
5000
0
12 mm
14 mm
20 mm
0
50
100
150
TIME(μsec)

Figure A-1

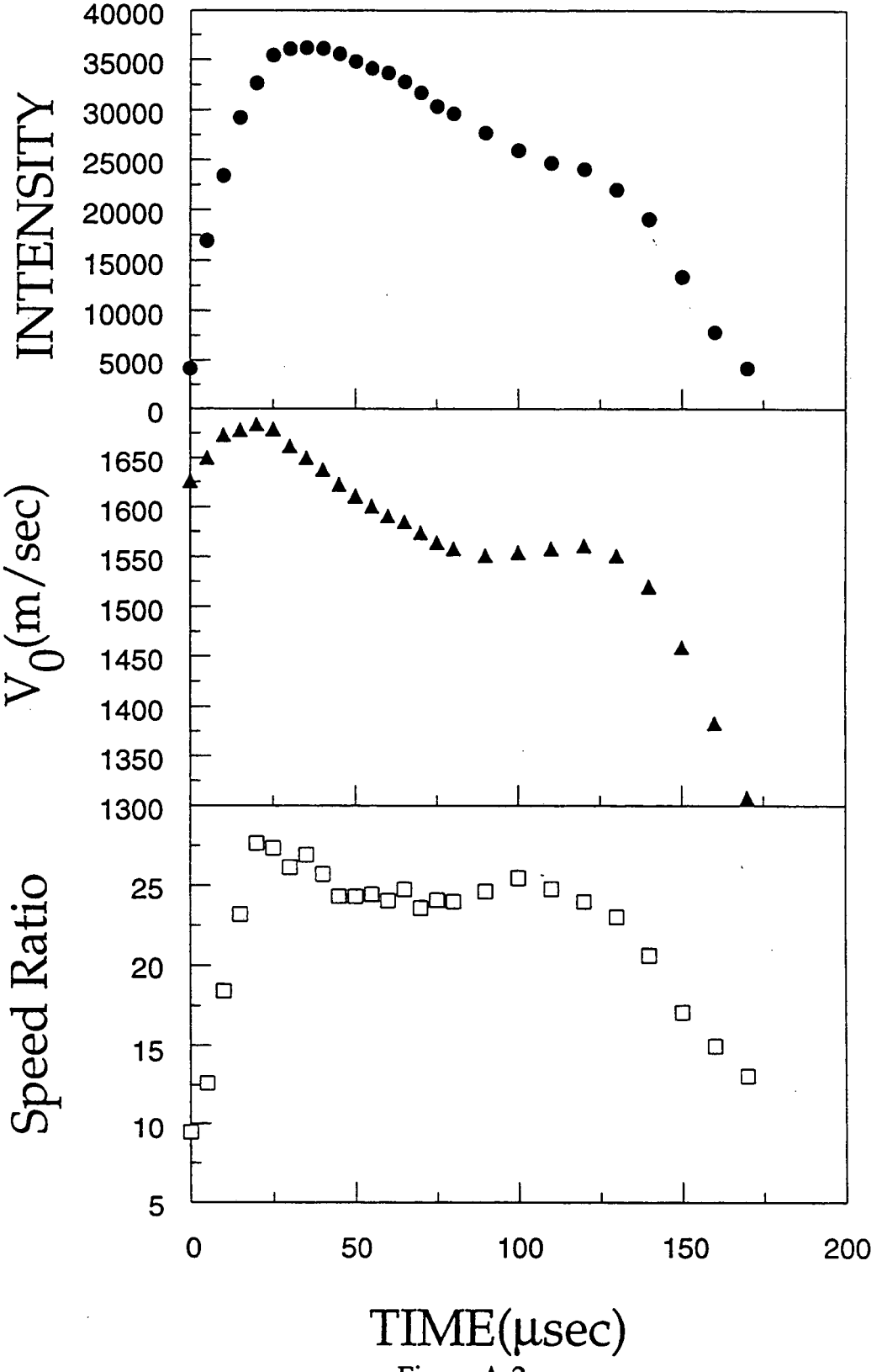
INTENSITY
40000
35000
30000
25000
20000
15000
10000
5000
0
V_0(m/sec)
1650
1600
1550
1500
1450
1400
1350
1300
Speed Ratio
25
20
15
10
5
0
50
100
150
200
TIME(μsec)

Figure A-2

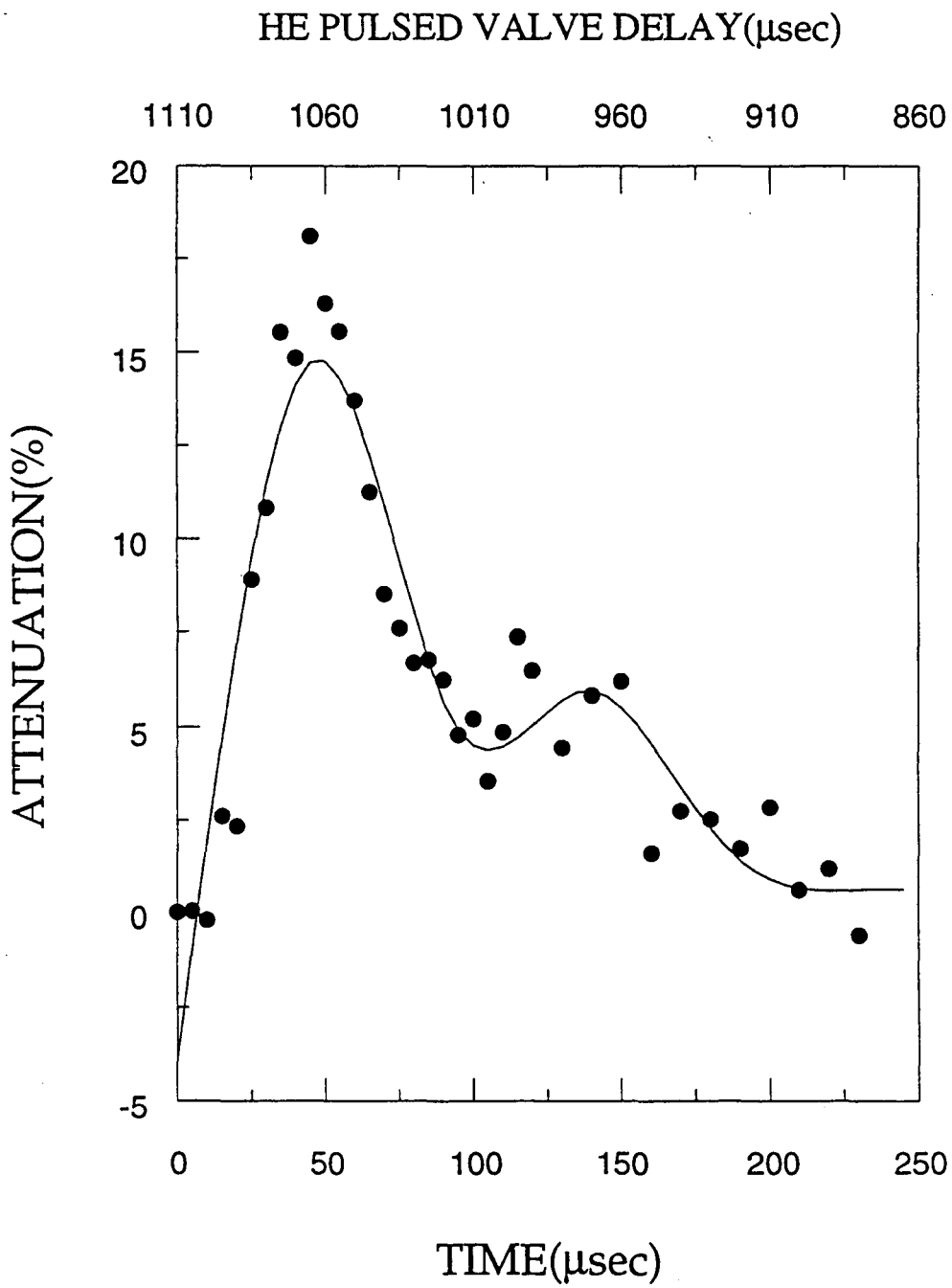
HE PULSED VALVE DELAY(μsec)
1110
1060
1010
960
910
860
20
15
10
5
0
-5
ATTENUATION(%)
0
50
100
150
200
250
TIME(μsec)

Figure B-1

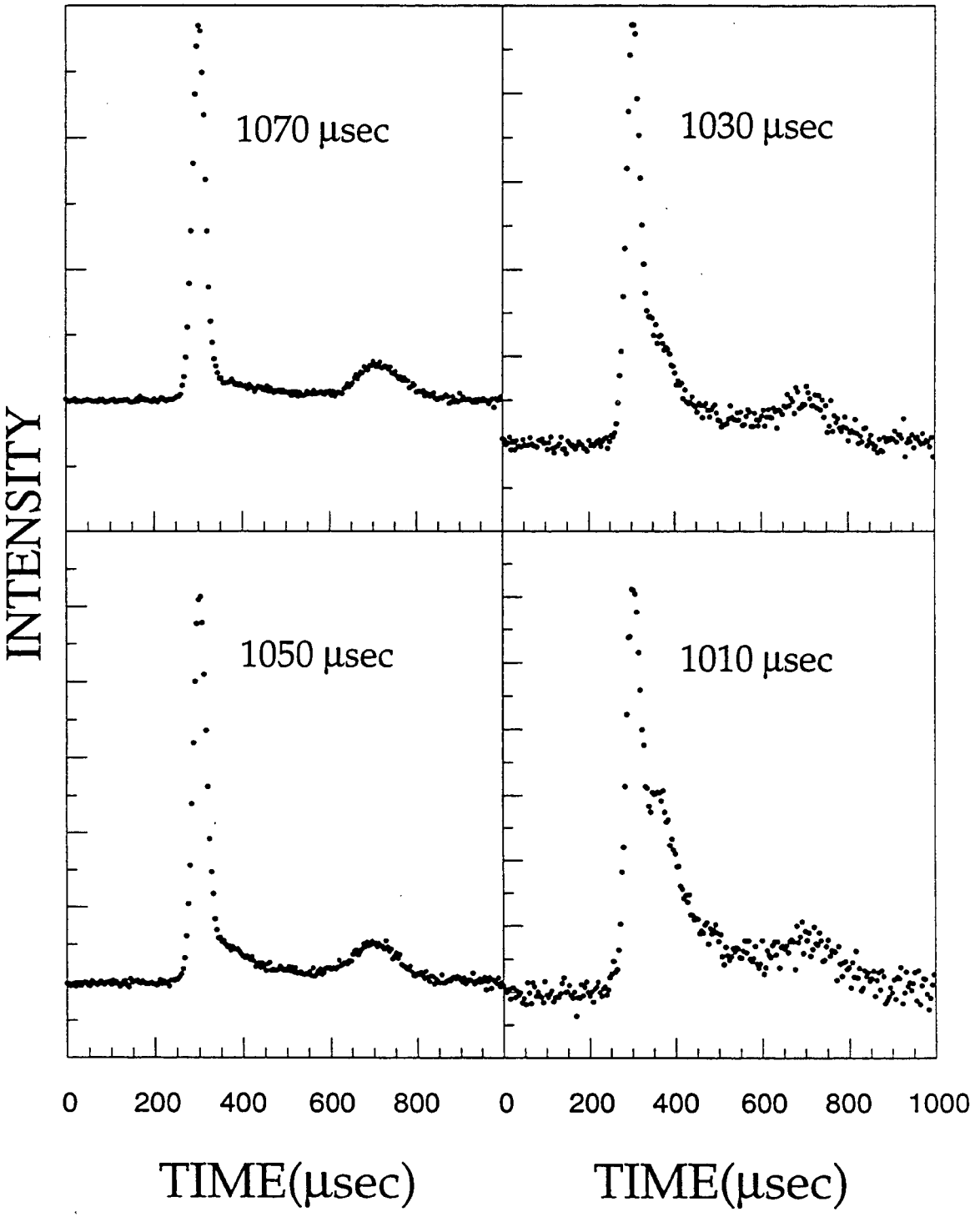
1070 µsec
1030 µsec
1050 µsec
1010 µsec
INTENSITY
0
200
400
600
800
0
200
400
600
800
1000
TIME(µsec)
TIME(µsec)

Figure B-2

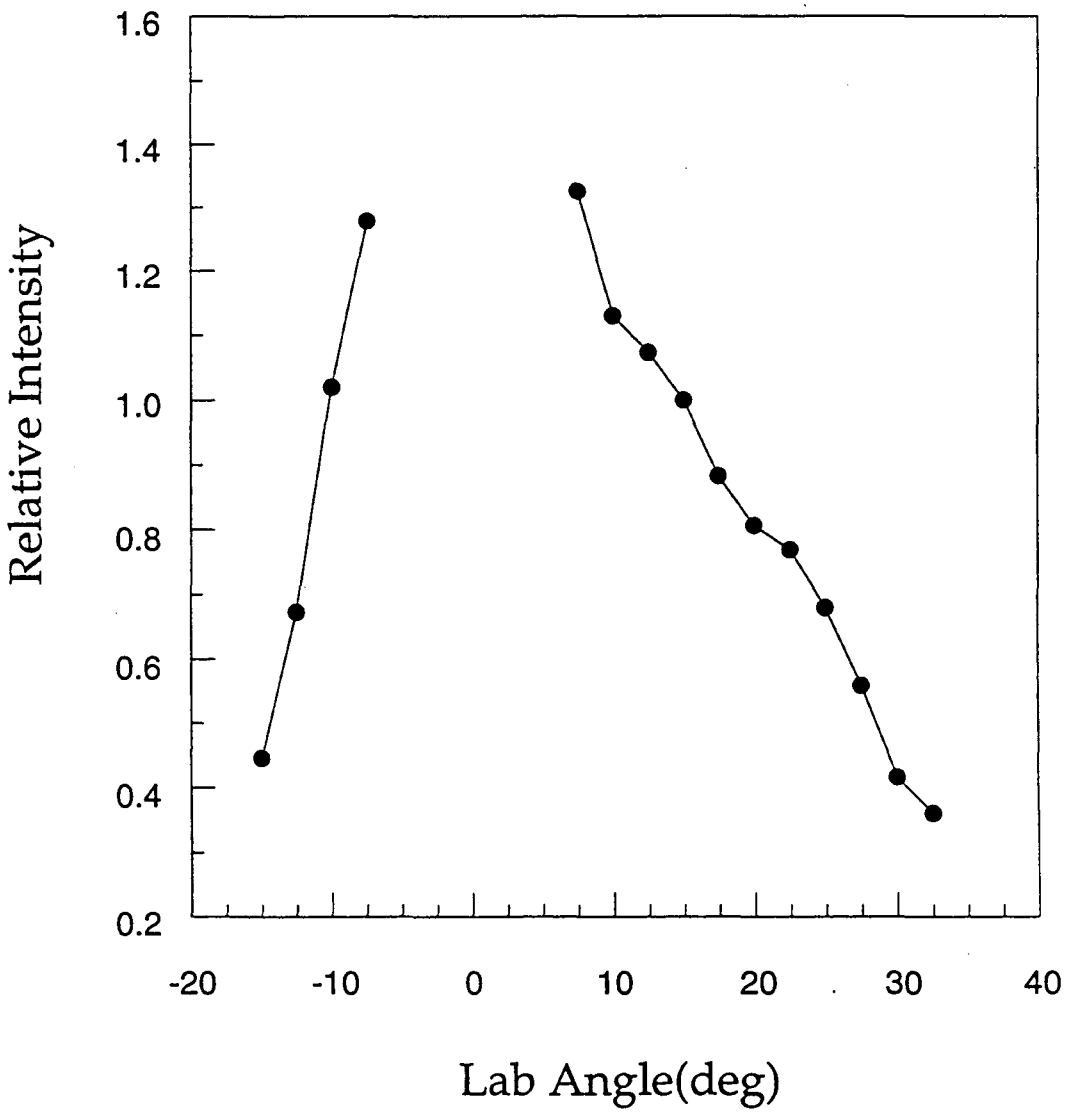
1.6
1.4
1.2
1.0
0.8
0.6
0.4
0.2
Relative Intensity
-20
-10
0
10
20
30
40
Lab Angle(deg)

Figure B-3

LAWRENCE BERKELEY LABORATORY
UNIVERSITY OF CALIFORNIA
TECHNICAL INFORMATION DEPARTMENT
BERKELEY, CALIFORNIA 94720